Joana Raquel Afonso Gomes

Degree in Biochemistry

Protein glycosylation of extracellular vesicles from ovarian carcinoma cells

Dissertation to obtain the Master Degree in
Biochemistry for Health

Supervisor: Júlia Carvalho Costa, Principal Investigator, ITQB

November, 2015

Joana Raquel Afonso Gomes

Degree in Biochemistry

Protein glycosylation of extracellular vesicles from ovarian carcinoma cells

Dissertation to obtain the Master Degree in
Biochemistry for Health

Supervisor: Júlia Carvalho Costa, Principal Investigator, ITQB

Jury:
President: Doctor Pedro Manuel Henriques Marques Matias
Opponent: Doctor Duarte Custal Ferreira Barral
Members of the jury: Doctor Júlia Carvalho Costa
Doctor Margarida Archer Baltazar Pereira da Silva Franco Frazão

Instituto de Tecnologia Química e Biológica

November, 2015

Copyright

Acknowledgments

It would not be possible to do this master thesis without the help and support of several people to whom I would like to express my sincere acknowledgments.

Firstly, I would like to thank to my supervisor, Dr. Júlia Costa, for the opportunity, for the guidance, for always being available and for all the scientific discussions that helped me to improve.

To Dr. Patrícia Alves for the kind help in the interpretation of mass spectrometry data.

To Dr. Cristina Peixoto and to Sofia Carvalho for the acquisition and interpretation of the NTA data.

To Daniel Simão for the help in obtaining the membrane fraction.

To my lab colleagues, Cláudia e Margarida, for being such good friends and for all the support in those days where science did not work as expected.

A todos os meus amigos de faculdade, em especial ao Filipe, por todas as palavras de incentivo e apoio ao longo deste ano. Obrigada por me fazeres rir com as tuas brincadeiras.

Às minhas amigas Filipa, Fátima e Catarina que apesar da distância e das conversas espaçadas me mostraram sempre, ao longo de todos estes anos, o verdadeiro significado do nosso lema 'Ser amiga é ser irmã'.

Ao Nuno. Obrigada por toda a tua paciência, carinho e apoio. Obrigada por me fazeres sorrir com as coisas mais simples e por me mostrares sempre o 'bright side of life' mesmo nos dias mais cinzentos.

À minha irmã, Gisela. Obrigada por seres a melhor amiga e companheira de aventuras e pelas tuas palavras encorajadoras, mesmo naqueles dias em que parecia não querer ouvir.

Por fim, ao meus pais, João e Manuela, a quem dedico esta tese. Obrigada por todos os sacrifícios feitos ao longo de tantos anos para que eu pudesse ser livre e tomar as minhas próprias decisões, obrigada pelo apoio incondicional em todas elas.

Preface

This work was performed in the Laboratory of Glycobiology of ITQB-UNL and funded by projects: ENMed/0001/2013, EURONANOMED II, Fundação para a Ciência e Tecnologia (FCT), Portugal; EU JPND Research, FCT, JPND/0003/2011; Pest-OE/EQB/LA0004/2011, FCT.

Joana Gomes is recipient of fellowship 007/BI/2015, from project ICV 342, ITQB.

Part of this work was published in Biomolecules: Gomes J, Gomes-Alves P, Carvalho SB, Peixoto C, Alves PM, Altevogt P, Costa J (2015). Extracellular Vesicles from Ovarian Carcinoma Cells Display Specific Glycosignatures *Biomolecules* 5:1741-61.

Part of this work was presented in a flash oral presentation and in a poster session in the "11th International Meeting of the Portuguese Carbohydrate Group and 6th Iberian Carbohydrate Meeting", September 2015, Viseu, Portugal.

Abstract

Extracellular vesicles (EVs) are released by almost all types of cells, including tumor, immune and stem cells, and are also present in body fluids like saliva, urine, breast milk and malignant ascites. EVs have a unique cargo of proteins, lipids and nucleic acids, and conserve characteristics from donor cells.

Herein, EVs and total cell membranes (MBs) were isolated from human ovarian carcinoma OVMz cells, and further characterized. EVs showed a strong enrichment in the specific EVs markers CD63, CD9 and Tsg101 and had an average size of 145 nm. On the other hand, MBs fraction contained markers of cellular organelles, including, calnexin (endoplasmic reticulum), GRASP65 and GS28 (Golgi apparatus), LAMP-1 (lysosomes) and L1CAM (plasma membrane).

The glycoprotein galectin-3 binding protein (LGALS3BP) was found to be strongly enriched in the EVs fraction where it was identified by mass spectrometry (MALDI-TOF/TOF), after trypsin digestion, and by immunoblotting. Digestion with endoglycosidase H, peptide N-glycosidase F and sialidase showed that LGALS3BP contained complex N-glycans with sialic acid.

The MBs and EVs glycan profiles were compared by lectin blotting, with a panel of lectins. EVs displayed specific glycosignatures relatively to MBs, with enrichment in α2,3-linked sialic acid, fucose and bisecting GlcNAc-containing glycoproteins. Glycoproteins with the LacdiNAc motif and O-glycans with the T-antigen were also detected.

The inhibition of the processing of high mannose to complex/hybrid N-linked glycans with the α-mannosidase I inhibitor, kifunensine, caused changes in the EVs composition including decreased levels of the glycoproteins L1CAM, CD63, CD9 and LGALS3BP but also the non-glycosylated protein Tsg101.

In conclusion, the isolated vesicles were enriched in specific EVs markers including the sialoglycoprotein LGALS3BP. Furthermore, the results showed that glycosignatures of EVs were specific and altered glycosylation within the cell affected the composition and/or dynamics of EVs release. Altogether, these results could provide potential novel biomarkers for ovarian cancer.

Keywords – glycosylation; extracellular vesicles; ovarian cancer; galectin-3-binding protein; kifunensine; biomarkers.

Resumo

As vesículas extracelulares (EVs) são libertadas por quase todos os tipos de células, incluindo células tumorais, e estão também presentes em fluidos corporais.

Neste trabalho, foram isoladas e caracterizadas frações de EVs e de membranas celulares (MBs) provenientes da linha celular humana de carcinoma do ovário, OVMz. Na fração de EVs observou-se um enriquecimento nas proteínas CD63, CD9 and Tsg101, marcadores específicos de EVs, e as vesículas apresentaram um tamanho médio de 145 nm. Na fração de MBs foi observada a presença de marcadores de organitos celulares, sendo estes calnexina (retículo endoplasmático), GRASP65 e GS28 (complexo de Golgi), LAMP-1 (lisossomas), L1CAM (membrana plasmática).

Na fração de EVs observou-se um forte enriquecimento da glicoproteína "galectin-3 binding protein" (LGALS3BP) a qual foi identificada por espectrometria de massa (MALDI-TOF/TOF) e por "immunoblotting". As digestões com endoglicosidase H, péptido N-glicosidase F e sialidase mostraram que a LGALS3BP continha N-glicanos do tipo complexo com ácido siálico.

Os perfis de glicosilação das frações de EVs e de MBs foram comparados por "blotting" de lectinas. A fração de EVs demonstrou ter um perfil de glicosilação específico e distinto, com enriquecimento em glicoproteínas contendo ácido siálico na ligação α2,3, fucose e "bisecting" GlcNAc. Foi também detectada a estrutura LacdiNAc e o antigénio-T.

A inibição do processamento de N-glicanos do tipo oligomanose para o tipo complexo/híbrido, com o inibidor "kifunensine", provocou alterações na composição da fração de EVs, reduzindo os níveis das glicoproteínas L1CAM, CD63, CD9 e LGALS3BP e da proteína não glicosilada Tsg101.

Concluindo, a fração de EVs encontrava-se enriquecida em marcadores de EVs incluindo a sialoglicoproteína LGALS3BP. Os resultados mostraram ainda que os perfis de glicosilação das EVs eram específicos, tendo a alteração da glicosilação celular afectado a composição e/ou dinâmica da libertação de EVs. No seu conjunto, estes resultados poderão fornecer novos potenciais biomarcadores para cancro do ovário.

Palavras-chave – glicosilação; vesículas extracelulares; cancro do ovário; "galectin-3-binding protein"; "kifunensine"; biomarcadores.

Index

Index of figures

Index of tables

Abbreviations

AAL – *Aleuria aurantia* lectin
Asn – Asparagine
BCA – Bicinchoninic Acid
CA-125 – Cancer Antigen 125
CE – Cellular Extract
Con A – Concanavalin A
ECL – *Erythrina cristagalli* lectin
EDTA – Ethylenediamine Tetraacetic
Endo H – Endoglycosidase H
EOC – Epithelial Ovarian Cancer
E-PHA – *Phaseolus vulgaris* erythroagglutinin
ER – Endoplasmic Reticulum
ESCRT – Endosomal Sorting Complex Required for Transport
EVs – Extracellular Vesicles
FIGO – Federation of Gynecology and Obstetrics
Fuc – Fucose
Gal – Galactose
GalNAc – N-Acetylgalactosamine
GlcNAc – N-Acetylglucosamine
GlcNAcT – N-Acetylglucosaminyltransferase
GclNAcT III – β1,4-N-Acetylglucosaminyltransferase III
GlcNAcT V – β1,6-N-Acetylglucosaminyltransferase V
HRP – Horseradish Peroxidase
ILVs – Intraluminal Vesicles
KIF – Kifunensine
Lac – Lactose
MAL – *Maackia amurensis* lectin
MBs – Total Cell Membranes
MVBs – Multivesicular Bodies
NTA – Nanoparticle tracking analysis
PBS – Phosphate-Buffered Saline
PBST – Phosphate-Buffered Saline with 0.1% (w/v) Tween-20
PNA – Peanut agglutinin
PNGase F – Peptide N-glycosidase F
PTM – Post-Translational Modification
Ser – Serine
SNA – *Sambucus nigra* agglutinin
Thr – Threonine
TBS – Tris-Buffered Saline
TBST – Tris-Buffered Saline with 0.1% (w/v) Tween-20
WGA – Wheat germ agglutinin
WFA – *Wisteria floribunda* agglutinin
α-MM – methyl-α-D-mannopyranoside

1. Introduction

1.1 Ovarian Cancer

Ovarian cancer is the seventh most common type of cancer among women and the eighth in terms of cancer related deaths. In developed countries in particular, it rises to sixth in terms of overall mortality, being also the most lethal gynecological cancer (Torre et al. 2015).

Ovarian cancer is a very heterogeneous disease that can originate from three different types of cells: epithelial, stromal endocrine and germ cells, resulting in distinct types of cancer. The most common type is epithelial ovarian cancer (EOC) that represents 90% of the malignant cases. The disease also presents different histological subtypes: serous, mucinous, endometrioid, clear cell, transitional cell, mixed and undifferentiated, where the subtype serous is the most usual with 75% of the cases (Jelovac and Armstrong 2011).

According to the International Federation of Gynecology and Obstetrics (FIGO), ovarian cancer progression can be classified by its localization (Table 1.1).

Table 1.1 – Guidelines for ovarian cancer staging from FIGO (adapted).

Stage I	Tumor is confined to ovaries.
Stage II	Tumor involves one or both ovaries with pelvic extension (below the pelvic brim) or primary peritoneal cancer.
Stage III	Tumor involves one or both ovaries with cytologically or histologically confirmed spread to the peritoneum outside the pelvis and/or metastasis to the retroperitoneal lymph nodes.
Stage IV	Distant metastasis excluding peritoneal metastasis.

A key factor to a positive therapeutic outcome is the stage at which the disease is detected. When diagnosed at early stages (stages I and II), the 5-year survival rate is between 80-90%, but at advanced stages (stages III and IV) these values drop drastically to around 20%. Although there are clear benefits from an early detection, doing so is very challenging due to the lack of specific symptoms, so in most cases, when discovered, ovarian cancer is already at an advanced stage - for example, for EOC, only 25% of the cases diagnosed are stage I (Gupta and Lis 2009, Aggarwal and Kehoe 2010).

Currently, screening is based on transvaginal ultrasound and measurement of the serum disease biomarker, cancer antigen 125 (CA-125). With the first one it is only possible to detect masses and alterations of the ovarian volume. However, it is not possible to distinguish between benign/malignant tumors (Karst and Drapkin 2010).

CA-125 is a mucin that is present in all healthy individuals, at low levels (< 35 U/ml), but in cases of ovarian cancer, there is a significant increase in the presence of this glycoprotein in the serum. This glycoprotein is used not only as a biomarker of the disease but also to monitor the response to the treatment, and to do the follow up of the patients once they finish it.

Although CA-125 is the most used biomarker to detect ovarian cancer in the clinic, it has some disadvantages associated with its sensitivity and specificity. For example, the

increase of CA-125 happens in about 80-90% of the cases of ovarian carcinoma but only 50% of the women with ovarian cancer, at an early stage, exhibit an increase in the mucin level. In terms of specificity, levels of CA-125 can be elevated by other conditions like: benign ovarian cysts, endometriosis, and pelvic inflammatory disease (Aggarwal and Kehoe 2010, Karst and Drapkin 2010).

Many studies related with the molecular and cellular mechanisms associated with cancer are performed with cell models cultivated *in vitro*. These have many advantages in tumor related studies where, for example, it is possible to have different cell lines representative of various stages and histotypes of the tumor. Moreover, tumor cell lines conserve the hallmarks of cancer, are easily propagated and it is possible to obtain reproducible results.

1.2 Protein glycosylation

1.2.1 Biosynthesis of glycans

Glycosylation is an important post-translational modification (PTM) of proteins and lipids that occur in all living beings. Almost all membrane and secreted proteins are glycosylated and this PTM is involved in many biological functions like: cell interactions with the microenvironment (cell proliferation, differentiation, migration, and adhesion), immune surveillance, inflammatory reactions, host–pathogen interactions and protein folding (Moremen et al. 2012, Christiansen et al. 2014)

Protein glycosylation can be of the N- or O-linkage type depending on the site where the glycan is bound. In N-glycosylation, the attachment of the oligosaccharide occurs to an asparagine (Asn) residue, in a consensus peptide sequence: Asn-X-Ser/Thr, commonly via N-acetylglucosamine (GlcNAc). N-glycans have a common pentasaccharide core region: Manα1-6(Manα1-3)Manβ1-4GlcNAcβ1-4GlcNAc1-Asn-X-Ser/Thr and can be divided in three main classes according to their structure: oligomannose or high mannose in which only mannose residues are attached to the core, complex that also contain other monosaccharide residues, including galactose, sialic acid and fucose, or hybrid in which only mannose residues are attached to the Manα1–6 arm of the core and one or two complex antennae are on the Manα1–3 arm (Fig. 1.1) (Varki et al. 2009).

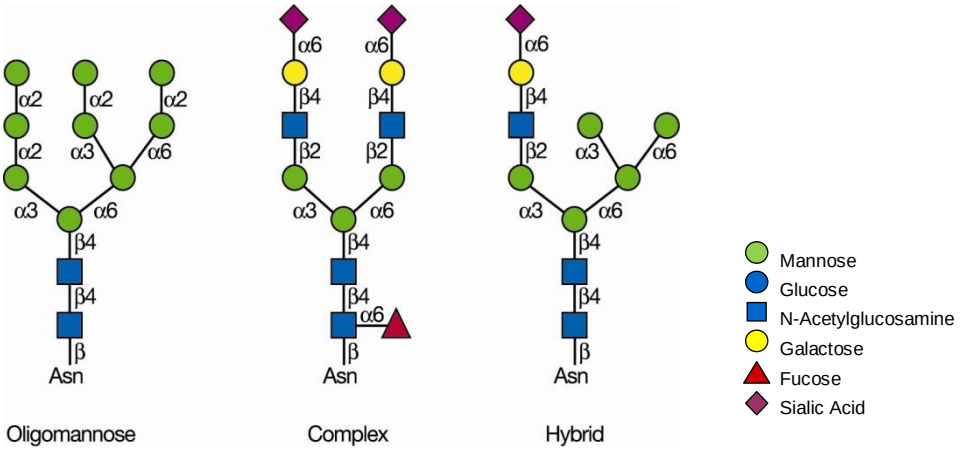

Figure 1.1 – Main classes of N-glycans. N-glycans share a common core region $Man_3GlcNAc_2$ and can be divided into three classes: oligomannose or high-mannose, complex and hybrid. After Varki et al. 2009.

In eukaryotes, the synthesis of N-glycans starts in the endoplasmic reticulum (ER) with the formation of the N-glycan precursor, a 14-sugar glycan ($Glc_3Man_9GlcNAc_2$), catalyzed by the action of specific glycosyltransferases. Then, this N-glycan precursor is transferred from dolichol phosphate to the nascent polypeptide chain, in a reaction catalyzed by oligosaccharyltransferase present in the ER membrane.

After this step, the processing of $Glc_3Man_9GlcNAc_2$ begins with the sequential removal of glucose residues by α-glucosidase I, II and the removal of terminal α1-2Man by the ER α-mannosidase I, yielding $Man_8GlcNAc_2$ isomer. In the cis-Golgi, trimming of α1–2Man residues are catalyzed by the action of α1–2 mannosidases IA, IB, and 1C, originating $Man_5GlcNAc_2$.

For the biosynthesis of complex and hybrid N-glycans, $Man_5GlcNAc_2$ is processed in medial-Golgi by the enzyme N-acetylglucosaminyltransferase I (GlcNAcT I). Next, the terminal α1-3Man and α1-6Man residues are removed by the enzyme Golgi α-mannosidase II, forming $GlcNAcMan_3GlcNAc_2$. Then, a second GlcNAc is added to the α1–6Man, in the core, by the action of GlcNAcT II, yielding the precursor for all biantennary, complex N-glycans. This precursor can be further processed by different enzymes like fucosyltransferase VIII (adds proximal fucose), galactosyltransferases (add galactose), sialyltransferases (add sialic acid), peripheral fucosyltransferases (add peripheral fucose) and N-acetylglucosamine transferases (add branches originating tri- and tetra-antennary N-glycans). In the synthesis of hybrid N-glycans, $GlcNAcMan_5GlcNAc_2$ is not processed by α-mannosidase II (Fig. 1.2) (Varki et al. 2009, Taylor and Drickamer 2011).

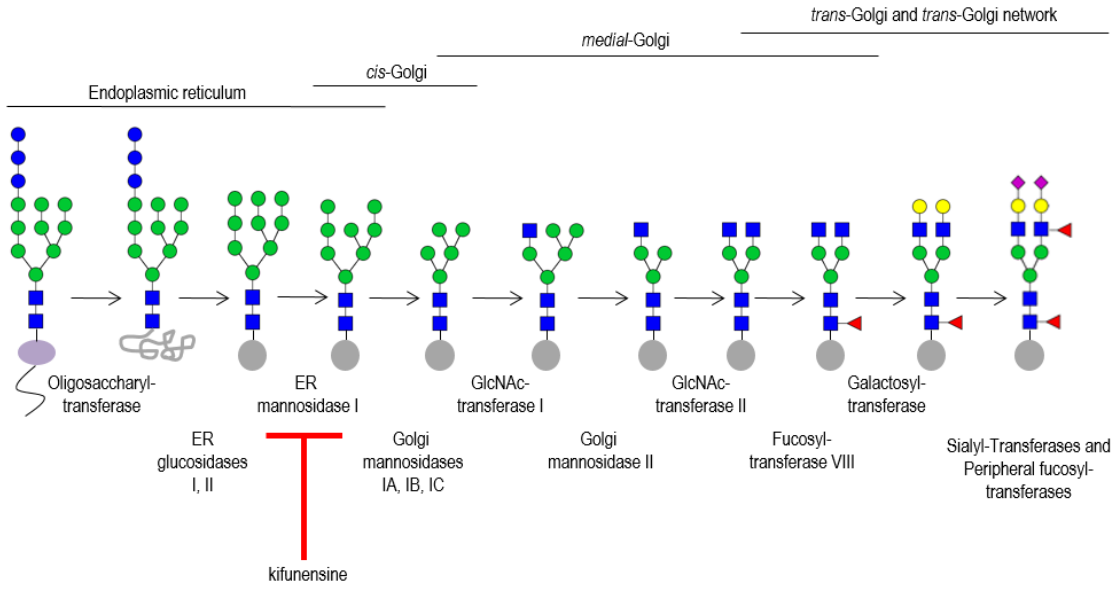

Figure 1.2 – Processing and maturation of N-glycans. N-glycans are processed in the ER and Golgi by different glycosyltransferases. After Taylor and Drickamer 2011.

In O-glycosylation, diversity is higher, mucin type O-glycans are attached to the peptide backbone on the hydroxyl group of a serine (Ser) or a threonine (Thr) residue, through N-acetylgalactosamine (GalNAc), a structure named Tn antigen. The most common O-GalNAc glycan is Galβ1-3GalNAc and it is termed T antigen. These two are only some examples of mucin type O-glycans with many other structures being found (Varki et al. 2009).

1.2.2 Glycosylation in cancer

Protein glycosylation is an important PTM for cell maintenance and survival. Overall, tumor cells present abnormal glycosylation patterns that can be caused by several factors like changes in the expression levels of glycosyltransferases, due, among other factors, to dysregulation at the transcriptional level, nucleotide sugar donor and substrate availability and localization of enzymes in secretory compartments (Stowell et al. 2015).

In cancer cells, one common alteration is the increase of β1,6 branching of N-glycans caused by augmented activity of the enzyme β1,6-N-acetylglucosaminyltransferase V (GlcNAcT V), coded by the gene *MGAT5*. This modification is associated with an enhanced capacity of the tumor to metastasize (Pinho and Reis 2015). An increase in invasion and metastasis was observed in mouse mammary cancer cell lines overexpressing the enzyme GlcNAcT V (Seberger and Chaney 1999).

Another common feature is an increase in fucosylation. Particularly, N- and O-glycans can carry α2,3/4-linked fucose residues originating the formation of Lewis blood group antigens ($Lewis^x$, $Lewis^y$, $Lewis^a$, $Lewis^b$), whose expression is elevated in several types of cancer like colon and breast cancer (Christiansen et al. 2014). Moreover, the $Lewis^x$ and $Lewis^a$ antigens can be sialylated with the addition of α2,3-linked sialic acid, generating sialyl-$Lewis^x$ and sialyl-$Lewis^a$ antigens. Both have been associated with cancer and expression of sialyl-$Lewis^x$ has been related with poor prognosis in cancer (Pinho and Reis 2015).

Bearing in mind the existence of distinct patterns of glycosylation between healthy and tumor cells, it is essential to study and compare them, in order to find new disease biomarkers and therapeutic targets. Lectins and antibodies are widely used reagents for the identification of glycan motifs. Lectins are glycan-binding proteins, with diverse origins, that are capable of binding specific glycan structures, with great affinity. On the other hand, antibodies are capable of recognizing determinants associated with cancer that lectins do not, like the Lewis blood group antigens. These two are used in diverse biochemical techniques like lectin/western blotting, histo/immunohistochemistry, flow cytometry and affinity chromatography (Varki et al. 2009).

Other techniques can be used for the study of cellular glycan composition like mass spectrometry. This technique has the possibility to discover new structures that are not identifiable by other methods referred above.

Another possibility is to measure enzyme's RNA expression, for example, glycosyltransferases mRNA, since altered enzymatic activity can have an effect in the glycan structure of a protein. Nevertheless, it is important to take in consideration that such structure is the result of the action of multiple enzymes involved in the glycan synthesis (Christiansen et al. 2014).

1.3 Extracellular vesicles

1.3.1 Characteristics

Extracellular vesicles (EVs) are released by almost all types of cells, including stem, immune and tumor cells, and are also present in body fluids like saliva, urine, breast milk and malignant ascites. They are a very heterogeneous group that contains vesicles with different cellular origins, sizes, morphology and composition (Colombo et al. 2014). EVs are typically classified by its size and origin, and there are three classes: exosomes, with an endosomal origin and a size between 30-150 nm, microvesicles resulting from the budding of the plasma membrane, size between 50-2000 nm and apoptotic bodies originating from the fragmentation of apoptotic cells with a size between 50 and 5000 nm (Vader et al. 2014).

The nomenclature of EVs has not been a consensual subject among the scientific community because there are several biophysical common characteristics between exosomes and microvesicles. Besides that, there is not an efficient and standardized protocol allowing the isolation of each type of EVs. The most used methodologies for EVs purification consists of successive low speed centrifugations followed by an ultracentrifugation, where the resulting pellet contains different EVs but possibly also unwanted protein aggregates (Colombo et al. 2014). Given the low efficacy of this purification process, other techniques have been employed based on the size of vesicles like density gradient centrifugation, where exosomes float between 1.13 and 1.19 g/ml, size exclusion chromatography, ultrafiltration and methods based in the biological composition of vesicles like immunoaffinity chromatography (Taylor and Shah 2015).

Isolated vesicles have been observed by electron microscopy where exosomes present a cup-shaped form but when observed by cryo–electron microscopy, these vesicles present a perfectly round shape. It is thought that this difference is due to the fixation/contrast step necessary for the EM protocol (Raposo and Stoorvogel 2013).

In terms of composition, EVs have a unique cargo of proteins, lipids and nucleic acids. Exosomes, due to their origin, have proteins that participate in the transport and fusion of the vesicles like Rab GTPases, SNAREs, annexins, flotillin, and that are involved in their biogenesis like Tsg101 and Alix. Exosomes are also enriched in tetraspanins, a family of proteins with four transmembrane domains, for example: CD63, CD9 and CD81 (Raposo and Stoorvogel 2013). Regarding lipid composition, in exosomes there is an enrichment in cholesterol, sphingomyelin, phosphatidylserine and saturated fatty acids. Concerning the composition in nucleic acids, exosomes present an enrichment in non-coding RNA (structural RNA, siRNA) and small RNA (mRNA and miRNA) with different sizes (Fig. 1.3) (Colombo et al. 2014). In the past few years, several studies concerning EVs composition have been performed. There is a database, Vesiclepedia (Kalra et al. 2012) (http://www.microvesicles.org/) that contains data on proteins, lipids and nucleic acids that are found on EVs.

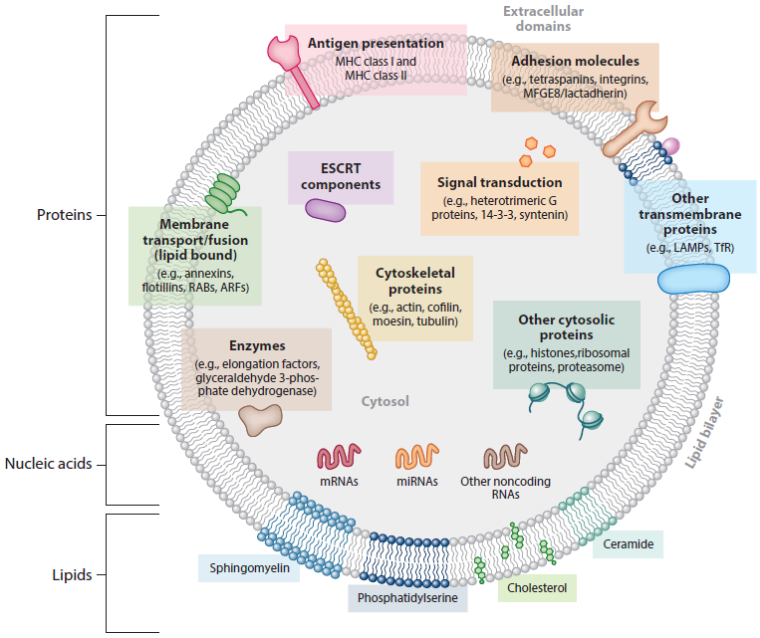

Figure 1.3 – Schematic representation of EVs composition. EVs have a diverse composition in proteins, lipids and nucleic acids. After Colombo et al. 2014.

1.3.2 EVs biogenesis

In the endocytic pathway, early endosomes are originated by the budding of the plasma membrane and then they evolve into late endosomes that can fuse with lysosomes or with the plasma membrane and release its contents outside the cell. During the maturation the limiting membrane of endosomes starts to invaginate towards the lumen, originating intraluminal vesicles (ILVs) that are inside multivesicular bodies (MVBs) and there is the accumulation of cytosolic proteins and lipids. In ILVs, the transmembrane proteins maintain the same topological orientation that they had in the plasma membrane. After all these processes, MVBs fuse with lysosomes or with the plasma membrane. If the second path occurs, ILVs are released outside the cell where they are designated as exosomes (Fig. 1.4) (Colombo et al. 2014, Kourembanas 2015).

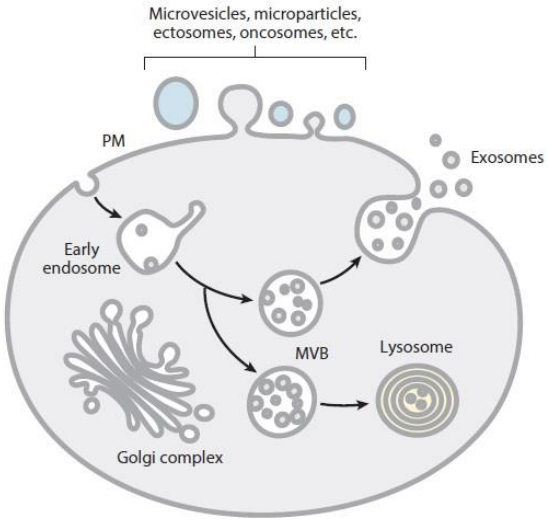

Figure 1.4 – Schematic representation of EVs subpopulations. Microvesicles formed by the budding of plasma membrane and exosomes that have an endosomal origin. After Colombo et al. 2014.

Exosome biogenesis can occur in different ways – one is dependent on the action of the endosomal sorting complex required for transport (ESCRT). This machinery has four complexes, ESCRT-0, ESCRT-I, ESCRT-II and ESCRT-III, which are responsible for this process. ESCRT-0 is a heterodimer formed by two subunits, HRS (hepatocyte growth factor-regulated tyrosine kinase substrate) and STAM 1/2 (signal transducing adaptor molecule). These two subunits have different motifs capable of binding phosphatidylinositol 3-phosphate, recognizing and sequestering monoubiquitinated cargo into the endosome and interacting with the complex ESCRT-I, through its protein Tsg101.

Therefore, ESCRT-0 recruits ESCRT-I, via Tsg101, and they are responsible for the monoubiquitinated cargo sorting into the MVBs, since ESCRT-I is also capable of recognizing ubiquitin. Besides Tsg101, ESCRT-I is formed by other subunits that recruit ESCRT-II and together, these two complexes are responsible for the membrane budding and stability (Babst 2011, Hanson and Cashikar 2012).

The complex ESCRT-III is distinct from the other three because it is formed by monomeric proteins that only assemble when recruited and this only happens by the interaction between the complexes –II e –III. Once assembled, ESCRT-III recruits the enzyme Doa4 (degradation of alpha 4) that is responsible for cargo deubiquitination. It is thought that complex ESCRT-III is responsible for neck constriction and vesicle scission. In the last step, complex ESCRT–III recruits the ATPase Vps4, leading to its own disassembling, in an energy consuming process, and this is crucial for the ESCRT machinery recycling (Henne et al. 2011, Hanson and Cashikar 2012, Kowal et al. 2014).

Recruitment to exosomes can also use a pathway independent of the ESCRT machinery which involves lipids, tetraspanins and heat shock proteins, which induce the inward curvature of MVBs (Kowal et al. 2014). In a study performed in oligodendroglial cells it was observed that the sorting of proteolipid protein to exosomes requires the synthesis of ceramide (Trajkovic et al. 2008). N-glycans can also be involved in the sorting of glycoproteins into the EVs. In a recent study, sorting of the glycoprotein EWI-2 into EVs, secreted by Sk-Mel-5 cells, was dependent on its N-glycan sites (Liang et al. 2014).

1.3.3 EVs in cancer

EVs have an important role in cellular communication since they carry information to adjacent or distant cells distinct from the one where they originated. Consequently, these vesicles participate in main biological functions like cell growth, differentiation (Marleau et al. 2012, Kourembanas 2015) and immune surveillance as they are capable of serving as antigen-presenting vesicles, stimulating anti-tumor effects or induce tolerogenic responses (Marleau et al. 2012). In order to deliver their content, EVs need to bind and to fuse with the recipient cells, a process that can occur in multiple ways and that is dependent on specific molecules present on the surface of EVs as well as the plasma membrane of target cells, most likely specific receptors and adhesion molecules. After binding, EVs can directly fuse with plasma membrane

or be internalized via the endocytic pathway where they fuse with the endosomal delimiting membrane, delivering their cargo (Raposo and Stoorvogel 2013, Colombo et al. 2014).

As referred above, tumor cells also release EVs that have been demonstrated to carry proteins associated with cancer (oncoproteins) and RNAs that contribute to tumor progression and metastasis, angiogenesis and immune suppression (Vader et al. 2014). In fact, evidence has demonstrated the presence of oncoproteins and RNAs that contribute to cancer development. EVs derived from a human squamous carcinoma cell line contain EGFR, and can transfer it to endothelial cells. Upon transfer, endothelial cells secreted elevated amounts of VEGF, a signaling molecule that contributes to angiogenesis (Al-Nedawi et al. 2009). In another study, glioblastoma derived EVs showed an enrichment in mRNA transcripts, compared to donor cells. Also, these same vesicles were capable to enter and to translate a reporter mRNA to brain microvascular endothelial cells (Skog et al. 2008).

Given the crucial role that EVs have in cancer, they have been proposed as potential biomarkers once they carry cargo that reflects characteristics of the donor cell. Another advantage is that EVs can be easily isolated from patients' blood. However, there is a technological challenge associated with EVs isolation and difficulties in distinguishing tumor derived EVs from EVs released by healthy cells (Vader et al. 2014). Recently, it was identified a surface proteoglycan, glypican-1, that was enriched in serum exosomes derived from patients with pancreatic cancer. The levels of this proteoglycan were correlated with tumor burden and showed a sensitivity and specificity of 100%, in each stage of the disease, being a potential biomarker (Melo et al. 2015). In ovarian cancer, it was observed that the protein cargo of exosomes varies among patients but in general display proteins associated with tumor growth like the protein EMMPRIN/CD147 (Keller et al. 2009). Another study, in ovarian cancer, described an increase in EVs circulating in the serum of patients and differences in the protein profile. EVs from patients showed an increase in TGF-β1 and MAGE 3/6 when compared with patients with benign tumors or healthy individuals (Szajnik et al. 2013).

Besides the EVs cargo, the analysis of EVs glycosylation is also a potential way to find new biomarkers since altered glycosylation is a common feature in cancer cells. A study concerning the glycosignatures of EVs purified from melanoma cells, colon cancer cells, T cells and breast milk showed that EVs had specific glycosignatures but they retained some characteristics of the parent cells (Batista et al. 2011). In an ovarian cancer cell line, purified exosomes exhibited enrichment of sialic acid-containing glycoproteins (Escrevente et al. 2011).

1.4 Thesis Objectives

The main objective of this work was to study the composition and glycosylation patterns of EVs secreted by OVMz cells, a human ovarian carcinoma cell line.

The first objective was the production and isolation of EVs from the OVMz cells. EVs were analyzed, by immunoblotting, to detect specific EVs markers, in order to confirm the identity of the isolated vesicles.

The second objective consisted in the analysis of MBs and EVs protein profiles, by SDS-PAGE, and the proteins enriched in each fraction were identified, after trypsin digestion, by MALDI-TOF/TOF.

The third objective consisted in the comparison of MBs and EVs glycosylation profiles, by lectin blotting, using nine different lectins. Since each lectin recognize a different glycan structures, it was possible to identify which glycan motifs were enriched in the EVs fraction.

The final aim was to evaluate the impact of glycosylation inhibition on EVs production and on the sorting of proteins into the vesicles. For this purpose the inhibitor kifunensine, which inhibits processing of high mannose to complex/hybrid N-linked glycans was used.

2. Material and Methods

2.1 Cell Culture and EVs production

The human ovarian cancer OVMz cell line was grown in Dulbecco's Modified Eagle Medium-High Glucose (Sigma), supplemented with 10% fetal bovine serum (Gibco), 100 units/ml penicillin and 0.1 mg/ml streptomycin (Gibco), at 37 °C, in 5% CO_2.

For cell counting, a Fuchs-Rosenthal chamber was used and for cell viability the trypan blue exclusion test was performed. This dye only crosses the plasma membrane of dead cells, so these cells are blue when observed at the microscope.

For the production of EVs, OVMz confluent cells were cultivated for 48 h in serum-free medium, to avoid contaminations by EVs from the bovine serum. The supernatant was collected and successively centrifuged at 500 and 10000x*g* for 10 and 20 min, to remove dead cells and cell debris, respectively. The supernatant was centrifuged at 100000x*g* for 120 min and the pellet consisted of the EVs fraction (Fig. 3.3). All the centrifugations were performed at 4 ºC (Escrevente et al. 2013).

For the study of glycosylation inhibition, kifunensine (KIF) (Sigma) was solubilized in serum-free medium and added to confluent cells, at 5 µM, for 48 h. Cells were grown in 24-well-plates to determine cell concentration and viability or in T75 flasks for EVs production. Statistical analysis was done using GraphPad Prism6 (GraphPad Software Inc.).

2.2 Protein quantification

Total protein concentration was determined by the bicinchoninic acid (BCA) method (Sigma) after protein precipitation with sodium deoxycholate and trichloroacetic acid to remove interfering compounds that could be present. The BCA method is based on the reduction of Cu^{2+} to Cu^{+} by the amino acids cysteine, tryptophan, tyrosine and by the peptide bond. The amount of Cu reduced is proportional to the amount of protein present. Then, BCA forms a blue-purple complex with the ions Cu^{+} that have an absorption maximum at 562 nm, allowing the quantification of total protein.

2.3 Preparation of cellular extract and total cell membranes fraction

To obtain cellular extract (CE), cells were collected with a cell scraper in phosphate-buffered saline (PBS) (10 mM $Na_2HPO_4.2H_2O$, 2 mM KH_2HPO_4 pH 7.2, 140 mM NaCl, 2.7 mM KCl) and centrifuged at 500x*g* for 5 min. Then, they were solubilized in 50 mM Tris-HCl pH 7.5, containing 5 mM ethylenediamine tetraacetic acid (EDTA), 1% (w/v) Triton X-100, 0.02% protease inhibitors cocktail, Complete (Roche) for 30 min, on ice. The extract was centrifuged at 10000x*g*, for 10 min, at 4 ºC, to remove insoluble material, and the supernatant corresponded to the CE fraction.

For the isolation of total cell membranes (MBs), confluent cells were incubated with 0.5 M EDTA pH 8.0, for 10 min, collected with a cell scraper and centrifuged at 500x*g*, for 5 min. Then, cells were sonicated on ice with 3 cycles of 5 seconds, at 70% power, Branson Digital Sonifier Models 250/450 and 2 min pause in between cycles on ice for cooling. MBs were

collected as the pellet of a 100000x*g* centrifugation, for 1 h (Pilobello et al. 2007). The diagrammatic representation of the procedures is shown in figure 3.3.

2.4 SDS-PAGE, immunoblotting and lectin blotting analysis

Proteins from MBs and EVs were analyzed by SDS-PAGE, in 10% acrylamide gels (T= 30.8%, C=2.6%). Proteins were solubilized in reducing sample buffer (0.08 M Tris-HCl pH 6.8, 2% SDS, 5% β-mercaptoethanol, 10% glycerol, 0.005% bromophenol blue) and incubated at 99 ºC, for protein denaturation. Gels were stained with Coomassie Blue R-250 (Merck) and destained with 25% methanol and 7% acetic acid.

For immunoblotting, proteins were separated by SDS-PAGE and transferred to polyvinylidene fluoride membranes. These were blocked for 1 h with 5% defatted dry milk (Nestlé) in PBS with 0.1% (w/v) Tween-20 (PBST) or in Tris-buffered saline (TBS) (20 mM Tris-HCl pH 7.5, 150 mM NaCl) with 0.1% (w/v) Tween-20 (TBST). Tween-20 was used to avoid non-specific binding of proteins to the polyvinylidene fluoride membrane. The membranes were incubated with the primary antibodies overnight, and with the secondary antibodies coupled to horseradish peroxidase (HRP) for 2 h. The incubation conditions and antibodies used are indicated in table 2.1.

Washings after the primary and secondary antibodies incubations were performed with PBST or TBST, four times, for 5 min.

Protein detection was performed with the Immobilon Western chemiluminescent HRP substrate (Millipore). This is based on the luminol oxidation, a reaction that emits light and it is catalyzed by peroxidase, coupled to the secondary antibody. Image acquisition was done in Chemidoc XRS$^+$ Imaging System (BioRad).

The conditions for lectin blotting with the lectins *Aleuria aurantia* lectin (AAL), *Erythrina cristagalli* lectin (ECL), peanut agglutinin (PNA), *Phaseolus vulgaris* erythroagglutinin (E-PHA), wheat germ agglutinin (WGA) and *Wisteria floribunda* (WFA) have been implemented in this work. The lectins Concanavalin A (Con A), *Maackia amurensis* lectin (MAL) and *Sambucus nigra* agglutinin (SNA) were used as previously described (Table 2.2) (Escrevente et al. 2011). Blots were blocked with 3% BSA biotin free (Carl-Roth) in TBST for 1 h, to avoid non-specific binding. They were incubated with each lectin, in the corresponding buffer, for 1 h and washed four times, 5 min.

Table 2.1 – Antibodies and incubation conditions used in immunoblotting analysis.

Antibodies	Dilution	Buffer	Conditions	Supplier
Goat anti-calnexin polyclonal	1:500	PBST	Reducing	Santa Cruz Biotechnology
Goat anti-GRASP65 polyclonal	1:500	PBST	Reducing	Santa Cruz Biotechnology
Goat anti-human LGALS3BP polyclonal	1:2000	PBST	Reducing	R&D
Goat anti-Tsg101 polyclonal	1:200	PBST	Reducing	Santa Cruz Biotechnology
Mouse anti-annexin-I monoclonal	1:5000	TBS	Reducing	BD Biosciences Pharmingen
Mouse anti-CD63 monoclonal	1:500	TBST	Non-reducing	Invitrogen
Mouse anti-CD9 monoclonal	1:5000	TBST	Non-reducing	Prof. Peter Altevogt, DKFZ, Germany
Mouse anti-EEA1 monoclonal	1:1000	TBST	Reducing	BD Transduction Lab
Mouse anti-GS28 monoclonal	1:250	TBST	Reducing	BD Transduction Lab
Mouse anti-human LAMP-1 monoclonal	1:500	TBST	Reducing	BD Biosciences Pharmingen
Mouse anti-L1CAM (L1-11A) monoclonal	1:1000	TBST	Reducing	Prof. Peter Altevogt, DKFZ, Germany
Rabbit anti-goat IgG coupled to HRP	1:20000	*	*	Sigma
Sheep anti-mouse IgG coupled to HRP	1:4000	*	*	Amersham

*The buffers used for the secondary antibodies were the same as for the corresponding primary antibodies.

Then, blots were incubated with 0.1 µg/ml streptavidin−peroxidase (Sigma) for 1 h and washed four times, for 5 min, with the corresponding buffer. Detection was performed with the Immobilon Western chemiluminescent HRP substrate (Millipore).

As control for non-specific binding, lectin incubations were done in the presence of competitive sugars: fucose (Fuc), methyl-α-D-mannopyranoside (α-MM), lactose (Lac), galactose (Gal), N-acetylgalactosamine (GalNAc) and N-acetylglucosamine (GlcNAc), after a pre-incubation of 15 min of the lectin with the sugar (Table 2.2).

To confirm MAL and SNA specificities, MBs and EVs were incubated with sialidase from *Vibrio cholerae* (Roche) that hydrolyzes α2,3- α2,6- and α2,8-linked neuraminic acid. The

reaction was carried out overnight, at 37 ºC, with 15 mU sialidase in 50 mM sodium acetate pH 5.5 containing 4 mM $CaCl_2$ (Escrevente et al. 2011).

Table 2.2 – Lectins, competitive sugars and conditions used in lectin blotting analysis.

Lectin	Concentration (µg/ml)	Salts	Supplier	Competitive Sugar
AAL	1	–	Galab Technologies	0.1 M Fuc
Con A	25	1 mM $CaCl_2$ + 1 mM $MnCl_2$	Sigma	0.1 M α-MM
ECL	0.5	1 mM $CaCl_2$ + 1 mM $MnCl_2$	Galab Technologies	0.5 M Lac
MAL	5	–	Galab Technologies	Incubation with *V.cholerae* sialidase
PNA	0.5	1 mM $CaCl_2$ + 1 mM $MgCl_2$	Galab Technologies	0.3 M Gal
E-PHA	0.5	1 mM $CaCl_2$ + 1 mM $MnCl_2$	Vector Laboratories	0.4 M GalNAc
SNA	0.5	–	Galab Technologies	Incubation with *V.cholerae* sialidase
WGA	0.1	–	Galab Technologies	0.5 M GlcNAc
WFA	1	–	Vector Laboratories	0.1 M GalNAc

2.5 Immunoprecipitation and deglycosylation of LGALS3BP

The protein LGALS3BP was immunoprecipitated from EVs solubilized in RIPA buffer (50 mM Tris-HCl pH 7.5, 150 mM NaCl, 0.1% SDS, 1% sodium deoxycholate, 1% (w/v) Triton-X 100, 0.02% protease inhibitors cocktail, Complete, Roche). First, the extract was pre-cleared by incubation with 20 µl of Protein A/G-agarose beads (Santa Cruz Biotechnologies) for 20 min, at 4 ºC, with constant rotation. This fraction was centrifuged at 10000*xg* for 5 min, at 4 ºC and the supernatant corresponded to the pre-cleared EVs fraction.

For each immunoprecipitation, 20 µl of Protein A/G-agarose beads were incubated with 5 µl of goat anti-human LGALS3BP polyclonal antibody (R&D) for 20 min, at 4 ºC, with constant rotation in RIPA buffer. Then, these beads were incubated for 1 h, at 4 ºC, with constant rotation, with the pre-cleared EVs. Washings were done with 250 µl RIPA buffer, three times, for 5 min.

For the deglycosylation of LGALS3BP, beads were incubated with 0.5% SDS, 1% β-mercaptoethanol and 0.02% protease inhibitors cocktail, Complete (Roche), for 10 min, at 99 ºC. After cooling, the beads were incubated at 37 ºC, overnight, either with 5 mU endoglycosidase H (Endo H; Roche) in 50 mM sodium citrate pH 5.5 or with 2.5 mU peptide N-glycosidase F (PNGase F; Prozyme) in 50 mM sodium phosphate pH 7.5 with 10 mM EDTA

and 1% (w/v) Nonidet P-40. For sialidase digestion, beads were incubated with neuraminidase from *Vibrio cholera*e in the conditions described above.

2.6 Nanoparticle tracking analysis

Concentration and size distribution of EVs were measured using a NanoSight NS500 (NanoSight Ltd). The samples were diluted in sterile PBS to get a particle concentration in the instrument linear range (10^8-10^9 particles/mL). All measurements were performed at 22 °C. Sample videos were analyzed with the Nanoparticle Tracking Analysis (NTA) 2.3 Analytical software – release version build 0025. Videos of 60-second were acquired and the average of ten measurements was considered as a representative result. Capture settings (shutter and gain) were adjusted manually. The mean size and standard deviation values of the major peak were calculated by taking into account all measurements.

2.7 MALDI-TOF/TOF analysis and protein identification

Following protein separation by SDS-PAGE, protein gel bands of interest were excised from the gel, destained with 50% (v/v) acetonitrile and digested overnight with trypsin (6.7 ng/µL) at 37 °C. Tryptic extracts were subsequently desalted, concentrated and were applied into a MALDI plate. Data were acquired in positive reflector MS and MS/MS modes using a 4800 plus MALDI-TOF/TOF (Applied Biosystems) mass spectrometer and the 4000 Series Explorer Software v.3.5.3 (Applied Biosystems). External calibration was performed using the calibration standards (Pepmix1; Laser BioLabs). The fifty most intense precursor ions from the MS spectra were selected for MS/MS analysis. Data were analyzed using Protein Pilot Software v. 4.5 (ABSciex) and the Mascot search engine (MOWSE algorithm). The search parameters used were: monoisotopic peptide mass values, maximum precursor mass tolerance (MS) of 50 ppm and a maximum fragment mass tolerance (MS/MS) of 0.3 Da; carbamidomethyl (C), deamidated (NQ), Gln- > pyro-Glu (N-term Q), and oxidation (M) as variable modifications. A maximum of two missed cleavages was allowed. The searches were performed against SwissProt protein database (547,357 sequences; 194,874,700 residues) with taxonomic restriction to *Homo sapiens* (20,200 sequences). Only MS/MS data were considered for protein identification. All proteins identified have at least: one peptide fragmented with a significant individual ion score (score > 32, $p < 0.05$) and a bold red peptide match, in order to eliminate duplicate homologous proteins. This work was performed by the Mass Spectrometry Unit (UniMS), ITQB/iBET, Oeiras, Portugal.

3. Results

3.1 Characterization of OVMz cell line

In this work, the human ovarian carcinoma cell line, OVMz, was used (Fig. 3.1), as an experimental cell model for ovarian cancer.

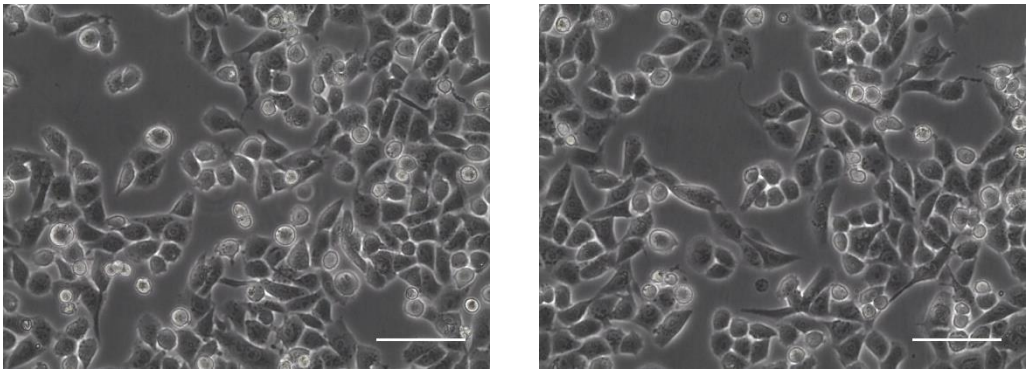

Figure 3.1 – Optical microscopy visualization of OVMz cells. The scale bar corresponds to 100 µm.

The growth of OVMz cells was monitored during five days and it is represented in figure 3.2. Cells were counted and cell viability was determined by the trypan blue exclusion test.

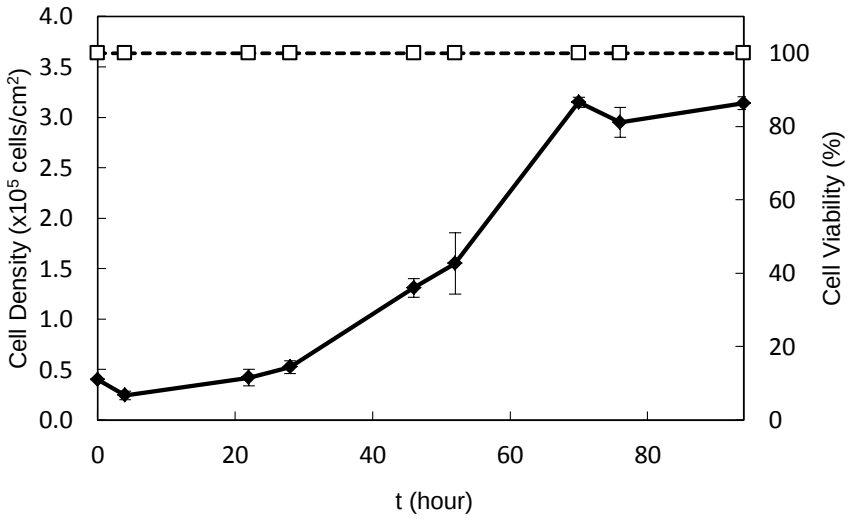

Figure 3.2 – Growth curve of OVMz cells. Cell density (closed symbols) and viability (open symbols) curves are presented. Results correspond to duplicates or triplicates and are presented as

Initially there was a decrease in cell density. This could be due to the cells not being adherent or being dead in suspension. After the second point (t=4 h) there was an increase and cells continued to grow during approximately three days. After that (t=70 h) cells entered a stationary phase in which they had already reached maximum confluence.

3.2 Isolation and characterization of EVs and MBs

EVs were isolated from OVMz confluent cells that were cultivated in serum-free medium, for 48 h. Cell viability was 99±1% (n=18), therefore, the absence of serum did not affect cell integrity. In this way, apoptotic vesicles were not significant contaminants of the EVs fraction.

The cell supernatant was collected and sequentially centrifuged at 500, 10000 and 100000*xg* for 10, 20 and 120 min, respectively (Fig. 3.3) (Escrevente et al. 2013). The amount of protein recovered was typically 130 µg/T175 as evaluated by the BCA quantification method.

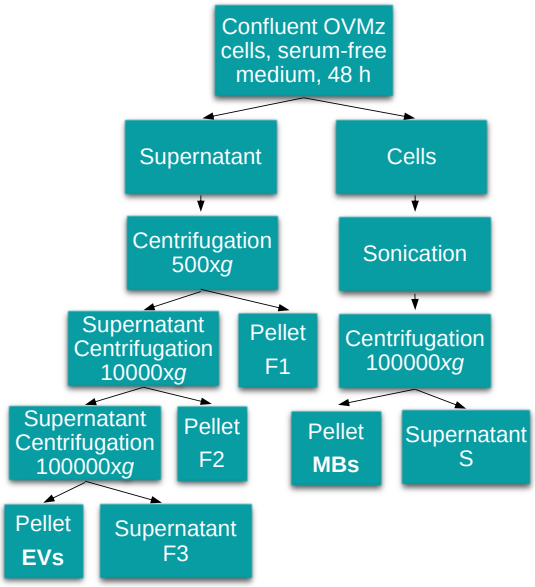

Figure 3.3 – Diagrammatic representation of the EVs and MBs isolation procedure.

The fractions recovered during the EVs isolation and the cellular extract were analyzed by immunoblotting to detect several EVs markers: CD63 (Escola et al. 1998, Lamparski et al. 2002), Tsg101 (Bobrie et al. 2012) found in exosomes (EVs from endosomal origin), CD9, described in microvesicles (EVs from plasma membrane budding) (Bobrie et al. 2012), L1CAM detected on the plasma membrane and exosomes (Stoeck et al. 2006), and LGALS3BP described in exosomes (Escrevente et al. 2013) (Fig. 3.4A). Here, the EVs fraction was strongly enriched in all these proteins, indicating that it contained microvesicles and exosomes.

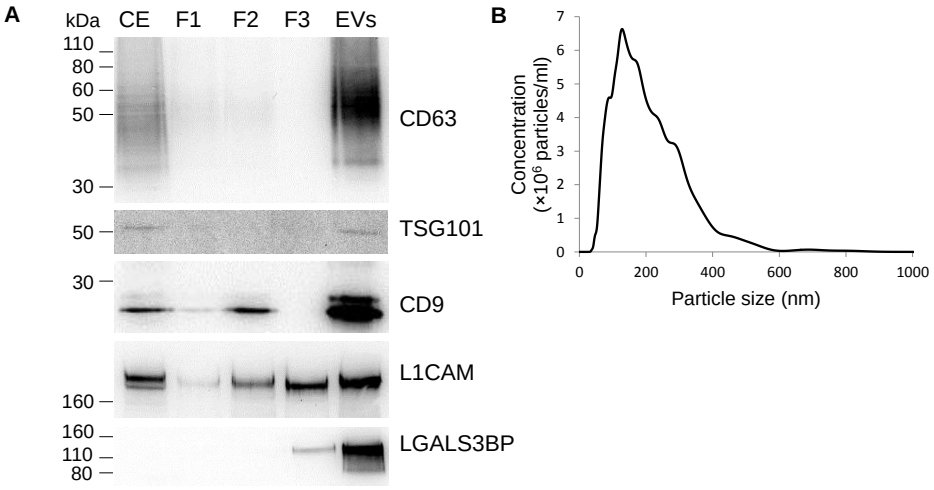

Figure 3.4 – Isolation of EVs from OVMz cells. (**A**) Immunoblotting of EVs markers in cellular extracts (CE), fractions collected during the purification (F1, F2, F3) and extracellular vesicles (EVs). Three µg of total protein were applied per lane with the exception of CE where ten µg of total protein were used. Detection was by the chemiluminescent method. Results were representative of two experiments; (**B**) NTA distribution profile of a representative population of EVs diluted in sterile PBS and analyzed using NanoSight NS500 equipment.

The EVs were also analyzed by NTA and a representative population is shown in figure 3.4B. The EVs fraction was diluted in sterile PBS in order to have a particle concentration of 10^8-10^9 particles/mL, within the instrument linear range. Taking in account all the measurements done, the population observed was very heterogeneous with sizes between 30 and 900 nm. The primary peak ranged between 91 and 191 nm and the mean average was 145±26 nm, n=24. The heterogeneity of the population is explained by the EVs isolation method used, an ultracentrifugation at 100000*xg,* which allows different subtypes of vesicles to co-sediment (Colombo et al. 2014).

Total cell membranes (MBs) were obtained for protein profile comparison with the EVs. MBs were isolated as a pellet of a 100000*xg* centrifugation, after cell sonication on ice. The MBs fraction was characterized by immunoblotting to detect proteins present in cellular membranes: L1CAM from the plasma membrane, calnexin from the endoplasmic reticulum, GRASP65 and GS28 from the Golgi apparatus, EEA1 from the early endosomes and LAMP-1 from the lysosomes (Fig. 3.5A).

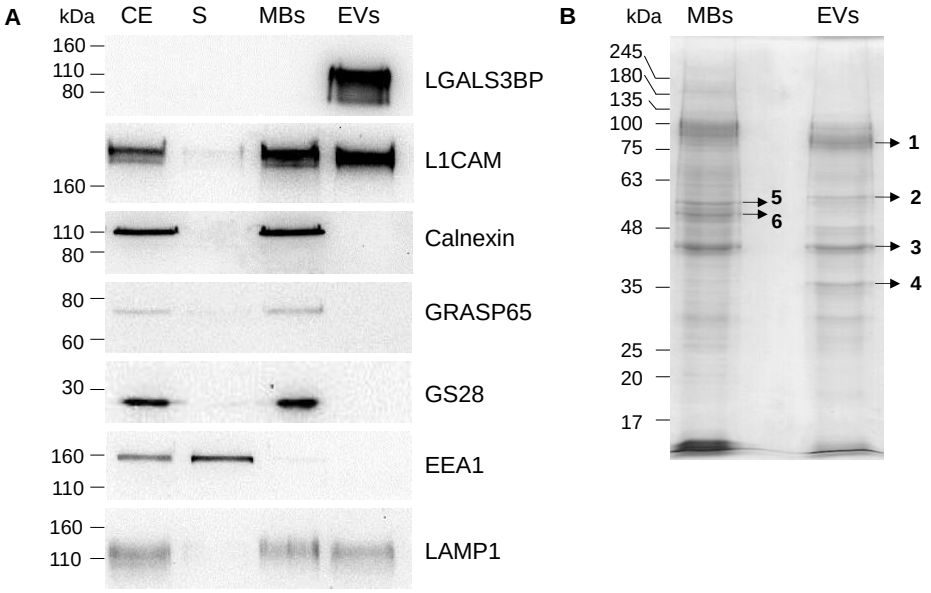

Figure 3.5 – Comparison of protein profiles of MBs and EVs from OVMz cells. (**A**) Immunoblotting of cellular extracts (CE), post-100000*xg* supernatant from MBs isolation (S), MBs and EVs. Ten µg of total protein were applied per lane with the exception of EVs in the incubation with LGALS3BP where three µg of total protein were used. Detection was by the chemiluminescent method. Results were representative of three experiments; (**B**) SDS-PAGE analysis of proteins of MBs and EVs. Ten µg of protein were applied per lane. Protein detection was with Coomassie R-250.

The MBs fraction was enriched in all the proteins tested indicating that this fraction contained membranes from different cellular organelles (Fig. 3.5A). For EEA1, the signal was more intense in the corresponding supernatant because EEA1 is a peripheral membrane protein, which was probably released by the sonication process. The protein LGALS3BP was not detected in the MBs fraction but was enriched in EVs.

3.3 MALDI-TOF/TOF

Proteins from MBs and EVs fractions were analyzed by SDS-PAGE and distinct protein profiles were observed (Fig. 3.5B). The protein bands enriched in each of the fractions were excised from the gel, digested with trypsin and identified by MALDI-TOF/TOF. The results are shown in table 3.1.

The extracellular matrix protein LGALS3BP was identified in the EVs fractions. This protein has a nominal mass of approximately 65 kDa but it appeared at around 110 kDa in the immunoblotting (Fig. 3.4A) since the protein is heavily glycosylated with seven N-glycosylation sites, which are occupied for truncated forms expressed in HEK293 cells (Hellstern et al. 2002). All the other identified proteins had a cytoplasmic origin and they were either cytoskeleton constituents (actin, tubulin, vimentin), present on MBs and EVs fractions, or enzymes (pyruvate kinase and glyceraldehyde-3-phosphate dehydrogenase), only identified on the EVs fraction. All proteins had already been previously identified in EVs (Vesiclepedia, http://microvesicles.org/).

3.4 LGALS3BP glycosylation

In order to study the glycosylation of LGALS3BP, this protein was immunoprecipitated from EVs fraction and deglycosylated with the enzymes: Endo H, PNGase F and *V. cholerae* sialidase. PNGase F hydrolyzes the bond between Asn and GlcNAc in all types of N-glycans. Endo H cleaves the bond between GlcNAcβ1-4GlcNAc only in oligomannose and hybrid N-glycans. *V. cholerae* sialidase hydrolyzes α2,3-, α2,6- and α2,8- linked N-acetylneuraminic acid (Fig. 3.6A).

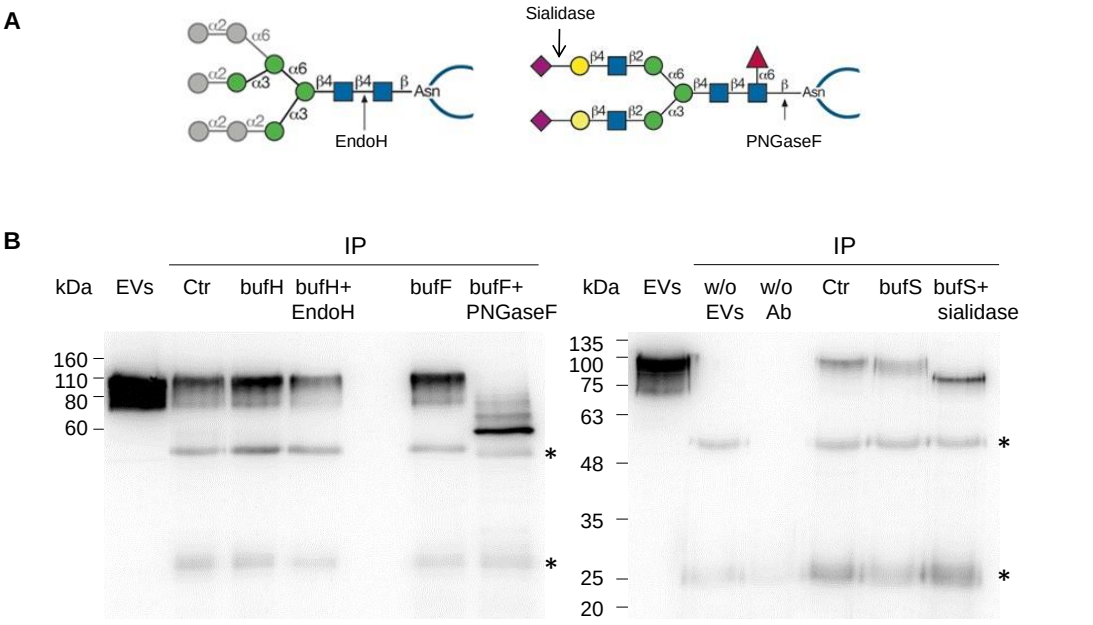

Figure 3.6 – Deglycosylation of immunoprecipitated LGALS3BP. (**A**) Schematic representation of enzymatic action of Endo H, PNGase F and *V.Cholerae* sialidase. (**B**) LGALS3BP was deglycosylated with Endo H, PNGase F, and *V. cholera* sialidase after immunoprecipitation from EVs (Ctr). The input EVs contained three µg of total protein. As control for the digestion the immunoprecipitate was incubated with the corresponding buffer (bufH for Endo H, bufF for PNGase F and bufS for sialidase). The controls of the immunoprecipitation without EVs (w/o EVs) and without antibody (w/o Ab) were also shown in the second panel. The blots are representative of two (Endo H) or four (PNGase F and sialidase) experiments. Immunoglobulin G bands are represented with *.

Table 3.1 – List of proteins identified in EVs and MBs from OVMz cells using MALDI-TOF/TOF after SDS-PAGE separation. Bands were excised from the gel shown in figure 3.5B. The data analysis was kindly performed by Dr. Patrícia Gomes-Alves.

Gel band	Protein name	UniProt identifier	Gene Name	Nominal mass (M_r)	Protein Score	Sequence coverage (%)	Queries Matched	Vesiclepedia
1	Galectin-3-binding protein	LG3BP_HUMAN	*LGALS3BP*	65289	460	27	13	+
	Alpha-actinin-4	ACTN4_HUMAN	*ACTN4*	104788	50	10	8	+
2	Pyruvate kinase PKM	KPYM_HUMAN	*PKM*	57900	47	18	7	+
3	Actin, cytoplasmic 2	ACTG_HUMAN	*ACTG1*	41766	447	50	15	+
	Actin, alpha cardiac muscle Actin, alpha skeletal muscle	ACTC_HUMAN ACTS_HUMAN	*ACTC1* *ACTA1*	41992 42024	166	19	7	+ +
4	Glyceraldehyde-3-phosphate dehydrogenase	G3P_HUMAN	*GAPDH*	36030	157	52	16	+
	Ezrin Moesin Radixin	EZRI_HUMAN MOES_HUMAN RADI_HUMAN	*EZR* *MSN* *RDX*	69370 67778 68521	69	3	3	+ + +
5	Vimentin	VIME_HUMAN	*VIM*	53619	415	48	21	+
6	Keratin, type II cytoskeletal 8	K2C8_HUMAN	*KRT8*	53671	84	21	12	+
	Tubulin alpha-1B chain	TBA1B_HUMAN	*TUBA1B*	50120	74	22	7	+
	Tubulin beta-4A chain Tubulin beta-4B chain	TBB4A_HUMAN TBB4B_HUMAN	*TUBB4A* *TUBB4B*	49554 49799	54	18	6	+ +

The results showed that controls of immunoprecipitation (w/o EVs and w/o Ab) were efficient since non-specific bindings were not detected. LGALS3BP was successfully immunoprecipitated from EVs fraction since a band at 110 kDa was observed on the immunoprecipitation control (Ctr) (Fig. 3.6B).

LGALS3BP was not deglycosylated by Endo H since the signal was similar to the control. Incubation with PNGase F caused a shift to a mass of approximately 60 kDa corresponding most likely to the fully deglycosylated form. Other bands less intense with superior molecular mass were also observed that could correspond to protein forms not fully deglycosylated or to another type of PTM. Digestion with *V. cholerae* sialidase also caused a downward shift of LGALS3BP indicating the presence of sialic acid. Altogether, these results indicate that LGALS3BP is a sialoglycoprotein with complex N-glycans (Fig. 3.6).

3.5 Glycosignatures of EVs and MBs

MBs and EVs glycan profiles were also compared by lectin blotting with nine different lectins (MAL, SNA, WGA, ECL, AAL, E-PHA, WFA, Con A and PNA). The lectins specificity is indicated in figure 3.7 below the blots. The results showed specific distinct glycosylation patterns between MBs and EVs (Fig 3.7).

EVs were enriched in glycoproteins containing α2,3-linked sialic acid, detected with MAL, and a strong band was observed at approximately 110 kDa. MAL binding was specific since it disappeared after sialidase digestion (Fig. 3.7A). The 110 kDa band consisted of LGALS3BP since immunoprecipitated LGALS3BP was detected by MAL (data not shown).

The cells did not contain glycoproteins with α2,6-linked sialic acid since the signal obtained with SNA was not specific as it persisted after sialidase incubation (Fig. 3.7A).

WGA, which binds sialic acid, also revealed a distinct profile between MBs and EVs, and a strong band appeared at approximately 110 kDa that is compatible with LGALS3BP. The glycoprotein profiles with ECL (that binds terminal galactose), AAL (peripheral and proximal fucose), E-PHA (bisecting GlcNAc), WFA (LacdiNAc structure), Con A (α-mannosyl containing branched glycans predominantly of the high-mannose followed by hybrid- and biantennary complex type structures to a lower extent), and PNA (T antigen) were also distinct between MBs and EVs fractions (Fig. 3.7B). Major bands that were enriched in EVs relatively to MBs and that decreased/disappeared in the presence of the competitive sugar are indicated on the right of the panels with arrowheads.

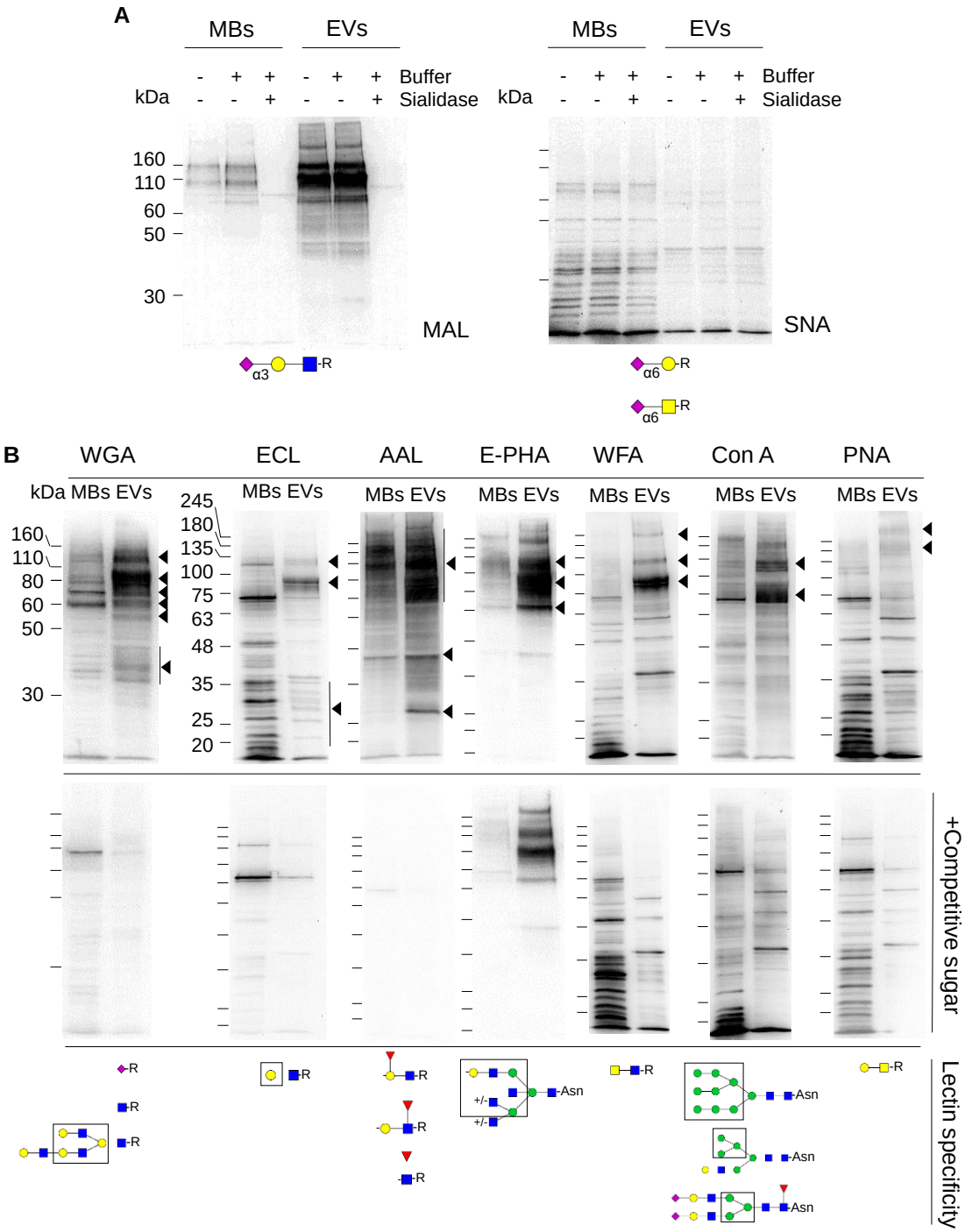

Figure 3.7 – Comparison of glycosignatures from MBs and EVs. (**A**) Lectin blotting with biotinylated MAL and SNA. As control for the lectin blotting, the samples were desialylated with *V. cholera* sialidase. (**B**) Lectin blotting with biotinylated WGA, ECL, AAL, E-PHA, WFA, and PNA, and non-biotinylated Con A (upper panels). Controls with competitive sugars as indicated in Material and Methods, are shown in the lower panels. Lectin specificities (Varki et al. 2009) are shown below the blots. Glycan representation is according to the nomenclature of the Consortium of Functional Glycomics. The lanes contained ten µg of total protein. Detection was by the chemiluminescent method. Major specific bands are indicated on the right with arrowheads. The blots are representative of at least three experiments.

3.6 Effect of kifunensine

Since EVs displayed specific glycosignatures (Fig. 3.7), the impact of glycosylation inhibition on EVs (glyco)protein composition was studied. In order to do that, confluent cells were cultured in serum free medium in the presence of 5 µM of KIF for 48h. KIF inhibits the enzyme α-mannosidase I causing the accumulation of $Man_{7-9}GlcNAc_2$, and leads to the absence of complex and hybrid N-linked glycans in glycoproteins (Varki et al. 2009).

Cell concentration, cell viability and total protein concentration of EVs fraction were measured, in the presence or absence of KIF (Table 3.2). Cell viability was not affected by the inhibitor. On the other hand, KIF caused a trend towards a decrease in cell concentration and an increase in total protein concentration in the EVs fraction but the differences were not statistically significant ($p>0.05$).

Table 3.2 – Effect of 5 µM KIF on cell concentration, cell viability and total protein concentration in EVs fraction.

	Control	KIF	p-value (unpaired t test)
Cell concentration (cells/well)	$6.1x10^5 \pm 0.5x10^5$ (n=6)	$5.4x10^5 \pm 0.6x10^5$ (n=6)	0.0662
Cell Viability (%)	99 ± 1 (n=18)	99 ± 1 (n=18)	–
Total protein concentration in EVs fraction (µg/T75)	48 ± 12 (n=8)	57 ± 3 (n=6)	0.0928

Proteins from the MBs and EVs fractions recovered in the absence (control) or presence (KIF) of KIF were analyzed by SDS-PAGE (Fig. 3.8A). The lane intensities were comparable and for LGALS3BP a downwards shift was observed indicating a transition from complex N-glycans to high mannose N-glycans. Indeed, high mannose N-glycans have lower molecular mass (e.g. $Man_9GlcNAc_2$ has 1883 Da) than complex glycans (e.g. complex sialylated diantennary with proximal fucose has 2369 Da or complex sialylated tetraantennary with proximal fucose has 3681 Da).

The effect of KIF on the recruitment of the glycosylated (CD63, LGALS3BP, L1CAM, CD9) and non-glycosylated (Tsg101, annexin-I) EVs markers into vesicles, was studied by immunoblotting (Fig. 3.8B). The KIF concentration efficiently inhibited glycosylation since for the glycoproteins CD63, LGALS3BP and L1CAM a downwards shift was observed which corroborates the results from figure 3.8A.

KIF caused a decrease in the intensity of the bands corresponding to CD63, LGALS3BP, L1CAM, CD9, Tsg101 and annexin-I (Fig. 3.8B). These results were supported by the values of the ratio KIF/control obtained from a semi-quantitative analysis of the immunoblottings (six replicates) (Fig. 3.8C). Particularly, the level of Tsg101 in EVs was the lowest whereas the level of annexin-I was the highest.

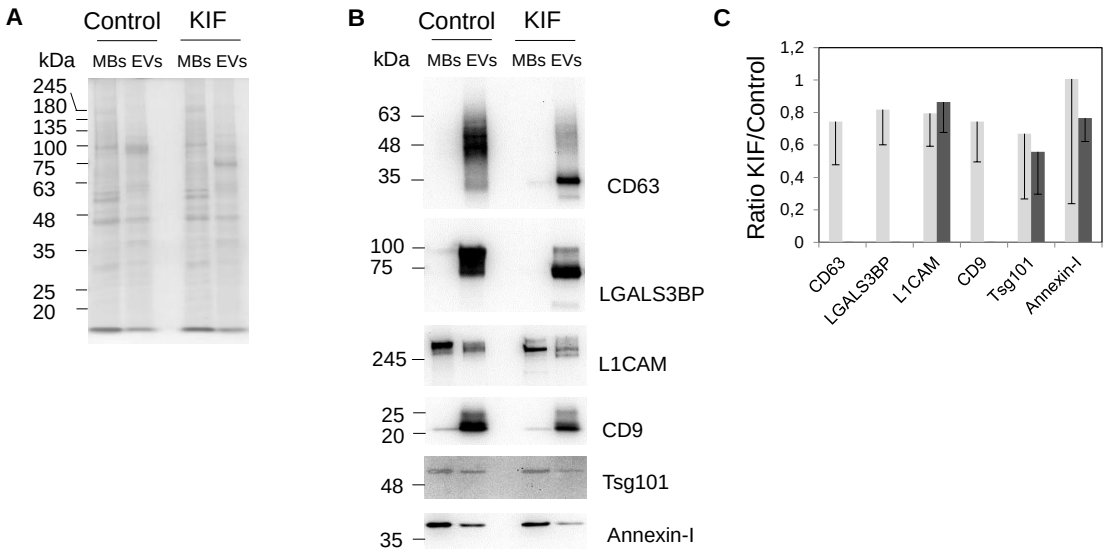

Figure 3.8 – Effect of kifunensine on the protein profiles from MBs and EVs. (**A**) SDS-PAGE analysis. Protein staining was with Coomassie Blue-R250. Five µg of total protein were applied per lane. KIF was used at 5 µM concentration; (**B**) Immunoblotting analysis. Three µg of total protein were applied per lane; (**C**) Semi-quantitative analysis of the ratio between band intensities in the presence or absence of KIF, using Image J software. Representative blots (B) average and standard deviation from six experiments are presented. Light and dark grey corresponded to EVs and MBs, respectively.

4. Discussion

Ovarian cancer is the most lethal gynecological cancer and its early detection is a key factor to a positive therapeutic outcome. The biomarker used in clinics, CA-125, lacks sensitivity since its levels are only increased in 50% of the women with ovarian cancer, at an early stage. Also, this marker is found overexpressed in other pathologies, thus hindering its specificity. Taking these in to account there is an urgent need to find novel biomarkers for ovarian cancer.

EVs can have an endosomal origin or be formed by plasma membrane budding. They are secreted by various cell types and are also present in biological fluids. These vesicles are important mediators of intercellular communication, carry information from cells and participate in many biological processes. As such, targeting EVs, in particular by studying protein cargo and patterns of glycosylation, which are altered in cancer, is now seen as a novel potential target of biomarker identification.

In this work, a human ovarian carcinoma cell line, OVMz, was used as an experimental model for ovarian cancer. The isolated EVs secreted by these cells were enriched in specific EVs markers and the vesicles population had an average size of 145 nm. Also, EVs displayed specific glycosignatures distinct from their parent cell membranes, with a strong enrichment in α2,3-linked sialic acid, fucose and bisecting GlcNAc. Finally, the inhibition of complex and hybrid N-linked glycans caused decreased levels of EVs markers, including glycoproteins into the vesicles.

4.1 EVs characterization and purification

EVs were isolated from confluent OVMz cells by sequential centrifugations. In order to confirm the identity of the isolated EVs and to monitor the isolation process, all the recovered fractions as well as the cellular extract were analyzed by immunoblotting to detect the following EV markers: CD63 (Escola et al. 1998, Lamparski et al. 2002), Tsg101 (Bobrie et al. 2012), CD9 (Lamparski et al. 2002), L1CAM (Stoeck et al. 2006) and LGALS3BP (Escrevente et al. 2013). The tetraspanin CD63 and Tsg101, proteins involved in exosome biogenesis, were particularly enriched in the EVs fraction and were also detected in the cellular extract. This result was expected since these two proteins are specific exosome markers.

The enrichment of the tetraspanin CD9 was also detected on the EVs fraction where two bands were observed (Fig. 3.4A). This indicated that different forms of CD9 probably with different post-translational modifications would be present in the EVs since this protein has two potential N-glycosylation sites and can be palmitoylated (Charrin et al. 2002). The tetraspanin CD9 is also a microvesicle (vesicles originated from the budding of the plasma membrane) marker and its presence on larger vesicles, pelleted at 10000*xg*, had previously been detected (Bobrie et al. 2012). Considering these facts, the presence of CD9 also in the F2 fraction was expected.

L1CAM was detected in the EVs fraction and also in all the remaining fractions with different intensities. L1CAM is a type I membrane glycoprotein with an ectodomain consisting of six Ig-like domains and five fibronectin-type III repeats. This ectodomain can be cleaved by

several enzymes in different locations converting the transmembrane protein into a soluble form (Mechtersheimer et al. 2001). A difference in migration of L1-CAM for F3 and EVs fractions was observed (Fig. 3.4A) so the L1CAM present in F3 could be a soluble form of this protein, resulting from the ectodomain cleavage. Moreover, in the cellular extract lane, two bands with molecular mass above 160 kDa were also detected indicating that different L1CAM forms could be present in this fraction. In fact, different L1CAM forms were detected in several cellular compartments and exosomes secreted by two ovarian cancer cell lines (Stoeck et al. 2006).

The glycoprotein LGALS3BP had previously been identified as exosome marker in SKOV3 ovarian cancer cells (Escrevente et al. 2013) and also other cells (Vesiclepedia, http://microvesicles.org/). In OVMz cells, an enrichment of this protein in the EVs fraction was also detected, by immunoblotting (Fig. 3.4A). LGALS3BP was also detected in the F3 fraction but not in the cellular extract. This protein is from the extracellular matrix and is capable of binding different cell surface proteins like collagens IV, V, VI, fibronectin, nidogen, integrin β1 and the lectin galectin-3 (Sasaki et al. 1998), which are all present in EVs (Vesiclepedia, http://microvesicles.org/). It is possible that LGALS3BP interacts with these proteins extracellularly explaining its presence in EVs and F3 fractions. However, further studies are necessary to understand the LGALS3BP localization and interactions on the EVs. One possibility could be the detection of LGALS3BP by imaging techniques including immunofluorescence microscopy of cells and electron microscopy with immunogold labeling of EVs.

Besides protein characterization, the EVs size was also determined by nanoparticle tracking analysis. A population of heterogeneous vesicles with an average size of 145 nm (n=24) was observed (Fig. 3.4B) and this result agreed with previous observations from other groups. EVs secreted by mouse skin melanoma cells (B16F10 cells) and HEK293T cells were isolated, by ultracentrifugation, and analyzed by NTA. The results showed that EVs secreted by both types of cells had a size range between around 50 and 300 nm (Nordin et al. 2015). On the other hand, in this work NTA analysis of OVMz derived EVs showed a size range between 30 and 900 nm, indicating the presence of several types of vesicles, with different sizes. This fact could be explained by the isolation method used since in the 100000*xg* pellet, different EVs subpopulations as well as protein aggregates, with similar sizes, could co-sediment as indicated in the literature (Colombo et al. 2014). In order to fine tune the isolation method, other isolation techniques could be explored such as density gradient centrifugation, size exclusion chromatography, ultrafiltration and methods based on the biological composition of vesicles like immunoaffinity chromatography (Taylor and Shah 2015). In fact, some studies have compared the differences between the possible isolation methods. One of them, compared ultracentrifugation with ultrafiltration with subsequent size-exclusion liquid chromatography. Using the last technique, a significantly higher EV yield was obtained and the vesicle protein composition was maintained (Nordin et al. 2015). In another study, EVs secreted by SKOV3 cells isolated by ultracentrifugation (crude exosomes) were compared to those further purified by sucrose gradient by electron microscopy. In both cases cup-shaped vesicles with

approximately 100 nm and smaller vesicles with a size between 30-50 nm were visible, however, in crude exosomes larger vesicles and vesicle aggregates were also observed (Escrevente et al. 2013). These results suggest that although a crude preparation of EVs can be isolated by ultracentrifugation, the method is not ideal to purify EVs subpopulations, such as exosomes.

Altogether, these results indicated that the fraction isolated by ultracentrifugation contained extracellular vesicles since it was enriched in specific EVs markers and the vesicle size agreed with reported results from the literature.

4.2 Protein sorting and glycosylation

The glycosylation patterns of EVs and MBs were compared by lectin blotting, using nine lectins with different specificities. The results showed that EVs displayed specific glycosignatures very distinct from their parent cell membranes. Previous results from the literature had already reported that EVs secreted by other cells, such as, T-cell lines (Jurkat, SupT1 and H9), colon cancer lines (HCT-15 and HT-29), skin cancer line (SkMel-5) (Batista et al. 2011) and SKOV3 ovarian cancer cells (Escrevente et al. 2011) had specific glycosignatures.

The EVs fraction showed an enrichment in glycoproteins with α2,3-linked sialic acid (recognized by MAL lectin) but glycoproteins with α2,6-linked sialic acid (recognized by SNA lectin) were not detected. These findings are distinct from previous ones where glycoproteins from SKOV3 ovarian cancer cells, had sialic acid in both types of linkage (Escrevente et al. 2011). This difference could be explained by the different cell line used. Major glycoproteins detected with MAL were also detected with WGA, which also recognizes sialic acid. Sialic acid has an important role in protein glycosylation since it is involved in different biological processes like cellular recognition, cell adhesion and cell signaling (Christiansen et al. 2014). In cases of cancer, increased expression of sialylated glycoproteins promotes the disruption of cell–cell adhesion, improving tumorigenesis (Pinho and Reis 2015).

Another structure that was found highly enriched in EVs was fucose as detected by AAL binding. Since AAL recognizes α1-2,-3, or -6-linked Fuc (Varki et al. 2009) but considering that OVMz cells did not express Lewis^y or Lewis^x antigens (Escrevente et al. 2006), then the signal obtained with AAL probably corresponded to proximal fucose (Fucα1-6GlcNAc). In agreement, no specific binding was detected with UEA lectin that recognizes Fucα1-2Gal (data not shown).

The bisecting GlcNAc structure, detected by E-PHA lectin, was specifically enriched in the EVs fraction. This structure had already been identified in human endometrioid ovarian cancer tissues (Abbott et al. 2008). It was also found in membrane proteins of serous ovarian cancer cell lines (Anugraham et al. 2014) and in human primary endometrioid and serous ovarian cancer tissues (Allam et al. 2015).

Glycoproteins with the LacdiNAc motif were also detected. This structure had already been found in the SKOV3 ovarian carcinoma cells (Machado et al. 2011). Moreover, glycoproteins with the T antigen from O-glycans were found.

Few glycoproteins were detected by the ECL lectin that recognizes Galβ1-4GlcNAc. One possible explanation for this low detection is that the lectin does not have access to the galactose due to the presence of α2,3-linked sialic acid on this residue.

Considering that EVs displayed specific glycosignatures, the importance of glycosylation on (glyco)protein sorting into the EVs was studied. In particular, the relevance of complex and hybrid glycans was investigated since these types of N-glycans were abolished in the presence of the α-mannosidase I inhibitor KIF. The sorting of the glycoproteins CD63, LGALS3BP, L1CAM, CD9 and the non-glycosylated proteins Tsg101 and annexin-I into the EVs was evaluated (Fig.3.8). A decrease in the levels of all these proteins in EVs was observed. However, this also happened for the proteins L1-CAM, Tsg101 and annexin-I from the MBs fraction. Considering that the total amount of protein applied per lane was the same in the absence or presence of KIF these results could suggest that the differences observed resulted from changes in the composition of EVs subpopulations. Since cell viability was not affected by KIF an increase in apoptotic vesicles would not be expected. Further studies are required to clarify if glycosylation plays a role in the recruitment of (glyco)proteins into EVs or if glycosylation inhibition changes the cell dynamics, altering the composition of EVs subpopulations.

Supporting the assumption that N-linked glycans participate in the protein sorting into the EVs, a recent study evaluated the effect of the α-mannosidase I inhibitor deoxymannojirimycin, on EVs secreted by the skin cancer cell line Sk-Mel-5. In this study, a reduction in the amount of the glycoprotein EWI-2 was observed in the EVs that were treated with the inhibitor, indicating that N-glycans may serve as determinants for EWI-2 recruitment into EVs. However, in that study a strong increase in the level of LGALS3BP was observed in EVs in the presence of the inhibitor, much in contrast to our findings (Liang et al. 2014). This may be explained by the different cell line used since the amount of LGALS3BP on EVs from Sk-Mel-5 cells is much lower than that observed in OVMz cells (Fig. 3.4A). All this body of evidence suggests that glycosylation may play a role in protein trafficking, particularly in the protein sorting into the EVs.

A possible glycoprotein sorting mechanism into EVs could involve galectins that are non-glycosylated lectins that specifically bind β-galactose-containing glycoconjugates (Varki et al. 2009). Galectin-3 which is raft-independent and galectin-4 which is associated with lipid domains, called ‘superrafts’, were found to be involved in the sorting of glycoproteins to the apical plasma membrane in polarized epithelial cells (Delacour et al. 2009). Also, it was found that the presence of α2,3 and α2,6-linked sialic acid on endolyn N-glycans mediates its apical delivery in MDCK cells, via a galectin-9–dependent mechanism (Mo et al. 2012).

The presence of galectins on EVs has been shown in several studies. Galectin-3 was detected in EVs isolated from skin and colon cancer cell lines (Sk-Mel-5 and HCT-15) (Batista et al. 2011, Liang et al. 2014). Also, galectin-4 was found to be present in EVs from T-cell line H9 and colon cancer cell line HT29 (Batista et al. 2011). Moreover, in another study, the presence of galectin-5 on the surface of rat reticulocyte exosomes was identified suggesting that this can

be contributing to selective sorting of N-acetyllactosamine-bearing glycoconjugates into exosomes (Barres et al. 2010).

The hypothesis to explain the involvement of lectins in glycoprotein sorting into EVs as a pathway complementary to the ESCRT pathway, would be that glycans interact with specific lectins, which promote the specific sorting of the carrier glycoproteins into exosomes or microvesicles at the endosome or at the plasma membrane, respectively. Whether that specific sorting would involve a previous enrichment into specific membrane domains (tetraspanin platforms or detergent resistant domains) could be a possibility. However, experimental evidence is still lacking at this point in support of these possible mechanisms.

4.3 EVs as cancer biomarker

The comparison of MBs and EVs protein profiles, showed the enrichment of some proteins. In particular, the extracellular matrix protein LGALS3BP was identified, in agreement with previous results by immunoblotting that showed its enrichment in the EVs fraction (Fig. 3.4A). This protein had already been detected in prostasomes (exosome-like vesicles secreted by the prostate) (Block et al. 2011), in SKOV3 ovarian cancer cells (Escrevente et al. 2013) and was also noted in Vesiclepedia (http://microvesicles.org/). In several tumors, this protein has been associated with a negative prognostic value, a shorter survival and the occurrence of metastasis (Grassadonia et al. 2004). The exact mechanism through which LGALS3BP contributes to cancer progression is still not clear but could involve its interactions with integrins, activating signaling transduction cascades involved in tumor progression (Stampolidis et al. 2015). The identification of specific proteins in tumor related EVs could be a strategy for discovery of novel cancer biomarkers. For example, in pancreatic cancer, the levels of glypican-1, from serum exosomes of patients, were recently correlated with tumor burden and showed a sensitivity and specificity of 100%, in each stage of the disease (Melo et al. 2015).

Specific glycan structures were found strongly enriched in EVs, namely α2,3-linked sialic acid, fucose and bisecting GlcNAc. Also, glycoproteins with the LacdiNAc motif were detected, which is in accordance with previous observations, since this structure was identified in ovarian cancer cells, SKOV3 (Machado et al. 2011). Furthermore, glycoproteins bearing O-glycans with T-antigen were also detected, and this structure is known to be increased in cancer (Pinho and Reis 2015).

In particular, bisecting GlcNAc had already been identified in glycoproteins from both human ovarian cancer cell lines and tissues (Abbott et al. 2008, Anugraham et al. 2014, Allam et al. 2015). Nine unique structures, containing bisecting GlcNAc were identified in membrane proteins of human cancer tissues but they were not found in control tissues (Allam et al. 2015). This evidence strongly suggested that bisecting GlcNAc could potentially be used as a biomarker for ovarian cancer.

Bisecting GlcNAc is synthesized by the enzyme β1,4-N-acetylglucosaminyltransferase III (GlcNAcT III), which is encoded by the gene *MGAT3*. In ovarian cancer, it has been proven that the gene *MGAT3* is overexpressed leading to an increase in bisecting N-linked structures

(Abbott et al. 2008). The gene overexpression could be due to epigenetic modifications such as DNA hypomethylation (Anugraham et al. 2014).

The presence of bisecting GlcNAc suppresses the existence of β1,6 – branching N-glycans, catalyzed by GlcNAcT V since both enzymes compete for the same substrate. In general, one typical modification that occurs in cancer cells is the increase of β1,6-branching structures that are strongly associated with tumor growth and progression (Dennis et al. 1987). Therefore, GlcNAcT III has been proposed as an antagonistic of GlcNAcT V that could contribute for tumor suppression. In fact, *MGAT3* expression inhibited the development of primary tumor lesions and tumor cell migration of cancer metastasis in mice carrying the mouse mammary tumor virus (Song et al. 2010). However, in ovarian cancer the mechanisms should be different since increased levels of bisecting-GlcNAc were observed in the tumor cells.

The study of EVs glycosylation as disease biomarker has also been a topic of interest in other diseases such as in neurological diseases, including ischemic stroke, multiple sclerosis and neurodegenerative disorders (Colombo et al. 2012). For example, lectin microarray technology was used to compare urinary EVs from individuals with autosomal dominant polycystic kidney disease to controls (Gerlach et al. 2013).

5. Conclusions

In this work, it was possible to isolate EVs secreted by OVMz cells by sequential centrifugations. The identity of the isolated vesicles was confirmed by the enrichment in the specific EVs markers CD63, Tsg101, CD9 and L1CAM and by their size. Furthermore, the sialoglycoprotein LGALS3BP was found abundantly enriched in EVs.

Moreover, it was demonstrated that EVs secreted by OVMz cells displayed specific glycosignatures distinct from their parent membrane cells. In particular, it was observed an enrichment in α2,3-linked sialic acid, fucose and bisecting GlcNAc and this last structure has been broadly associated with ovarian cancer.

The inhibition of the processing of high mannose to complex/hybrid N-linked glycans led to decreased levels of (glyco)proteins in the EVs, which could indicate that glycosylation inhibition affects the composition and/or the dynamics of EVs release.

Finally, the results obtained contributed to the identification of potential novel biomarkers for ovarian cancer.

6. Future perspectives

Considering that EVs displayed specific glycosignatures, an interesting possibility would be to perform a detailed characterization of EVs glycosylation. In order to do that, more powerful analytical techniques will be required, such as, high-performance anion exchange chromatography with pulsed amperometric detection and mass spectrometry (including MALDI-TOF/TOF), which will allow to have a complete structural information about the glycans present in the EVs glycoproteins. In addition, and from a clinical perspective, an interesting approach would be the study of the exosomes glycosignatures from serum patients, to confirm and possibly find new glycan structures associated with ovarian cancer.

Concerning EVs isolation procedures, it is still difficult to have a method capable of separating microvesicles from exosomes due to their biophysical common characteristics. In the future, a compelling possibility would be to explore other isolation techniques, including density gradient centrifugation and immunoaffinity chromatography. The isolation of EVs subpopulations would simplify, for example, studies related with the impact of glycosylation inhibition on the protein sorting into exosomes and on the dynamics of EVs release. Also, other glycosylation inhibitors, such as tunicamycin, which abolishes N-glycosylation and swansonine, which prevents the formation of complex N-linked glycans, could be explored in order to clarify the role of N-glycosylation in the sorting of (glyco)proteins into the EVs.

Bearing in mind that LGALS3BP is a protein from the extracellular matrix and it is present in the EVs and F3 fractions, studies concerning its localization and interactions with EVs surface proteins would be interesting. One option would be the use of imaging techniques like immunofluorescence microscopy of cells and immunogold labeling of EVs. Moreover, taking into account the enrichment of LGALS3BP in the EVs fraction and its seven N-glycosylation sites, another interesting approach would be the mutation of these sites in order to understand how the LGALS3BP glycosylation affects its recruitment into the vesicles.

7. References

Abbott KL, Nairn AV, Hall EM, Horton MB, McDonald JF, Moremen KW, Dinulescu DM, Pierce M (2008). Focused glycomic analysis of the N-linked glycan biosynthetic pathway in ovarian cancer. *Proteomics*. 8: 3210-3220.

Aggarwal P, Kehoe S (2010). Serum tumour markers in gynaecological cancers. *Maturitas*. 67: 46-53.

Al-Nedawi K, Meehan B, Kerbel RS, Allison AC, Rak J (2009). Endothelial expression of autocrine VEGF upon the uptake of tumor-derived microvesicles containing oncogenic EGFR. *Proc Natl Acad Sci U S A*. 106: 3794-3799.

Allam H, Aoki K, Benigno BB, McDonald JF, Mackintosh SG, Tiemeyer M, Abbott KL (2015). Glycomic analysis of membrane glycoproteins with bisecting glycosylation from ovarian cancer tissues reveals novel structures and functions. *J Proteome Res*. 14: 434-446.

Anugraham M, Jacob F, Nixdorf S, Everest-Dass AV, Heinzelmann-Schwarz V, Packer NH (2014). Specific glycosylation of membrane proteins in epithelial ovarian cancer cell lines: glycan structures reflect gene expression and DNA methylation status. *Mol Cell Proteomics*. 13: 2213-2232.

Babst M (2011). MVB vesicle formation: ESCRT-dependent, ESCRT-independent and everything in between. *Curr Opin Cell Biol*. 23: 452-457.

Barres C, Blanc L, Bette-Bobillo P, Andre S, Mamoun R, Gabius HJ, Vidal M (2010). Galectin-5 is bound onto the surface of rat reticulocyte exosomes and modulates vesicle uptake by macrophages. *Blood*. 115: 696-705.

Batista BS, Eng WS, Pilobello KT, Hendricks-Munoz KD, Mahal LK (2011). Identification of a conserved glycan signature for microvesicles. *J Proteome Res*. 10: 4624-4633.

Block AS, Saraswati S, Lichti CF, Mahadevan M, Diekman AB (2011). Co-purification of Mac-2 binding protein with galectin-3 and association with prostasomes in human semen. *Prostate*. 71: 711-721.

Bobrie A, Colombo M, Krumeich S, Raposo G, Thery C (2012). Diverse subpopulations of vesicles secreted by different intracellular mechanisms are present in exosome preparations obtained by differential ultracentrifugation. *J Extracell Vesicles*. 1.

Charrin S, Manie S, Oualid M, Billard M, Boucheix C, Rubinstein E (2002). Differential stability of tetraspanin/tetraspanin interactions: role of palmitoylation. *FEBS Lett*. 516: 139-144.

Christiansen MN, Chik J, Lee L, Anugraham M, Abrahams JL, Packer NH (2014). Cell surface protein glycosylation in cancer. *Proteomics*. 14: 525-546.

Colombo E, Borgiani B, Verderio C, Furlan R (2012). Microvesicles: novel biomarkers for neurological disorders. *Front Physiol*. 3: 63.

Colombo M, Raposo G, Thery C (2014). Biogenesis, secretion, and intercellular interactions of exosomes and other extracellular vesicles. *Annu Rev Cell Dev Biol*. 30: 255-289.

Delacour D, Koch A, Jacob R (2009). The role of galectins in protein trafficking. *Traffic*. 10: 1405-
1413.

Dennis JW, Laferte S, Waghorne C, Breitman ML, Kerbel RS (1987). Beta 1-6 branching of Asn-linked oligosaccharides is directly associated with metastasis. *Science*. 236: 582-585.

Escola JM, Kleijmeer MJ, Stoorvogel W, Griffith JM, Yoshie O, Geuze HJ (1998). Selective enrichment of tetraspan proteins on the internal vesicles of multivesicular endosomes and on exosomes secreted by human B-lymphocytes. *J Biol Chem*. 273: 20121-20127.

Escrevente C, Grammel N, Kandzia S, Zeiser J, Tranfield EM, Conradt HS, Costa J (2013). Sialoglycoproteins and N-glycans from secreted exosomes of ovarian carcinoma cells. *PLoS One*. 8: e78631.

Escrevente C, Keller S, Altevogt P, Costa J (2011). Interaction and uptake of exosomes by ovarian cancer cells. *BMC Cancer*. 11: 108.

Escrevente C, Machado E, Brito C, Reis CA, Stoeck A, Runz S, Marme A, Altevogt P, Costa J (2006). Different expression levels of alpha3/4 fucosyltransferases and Lewis determinants in ovarian carcinoma tissues and cell lines. *Int J Oncol*. 29: 557-566.

Gerlach JQ, Kruger A, Gallogly S, Hanley SA, Hogan MC, Ward CJ, Joshi L, Griffin MD (2013). Surface glycosylation profiles of urine extracellular vesicles. *PLoS One*. 8: e74801.

Grassadonia A, Tinari N, Iurisci I, Piccolo E, Cumashi A, Innominato P, D'Egidio M, Natoli C, Piantelli M, Iacobelli S (2004). 90K (Mac-2 BP) and galectins in tumor progression and metastasis. *Glycoconj J*. 19: 551-556.

Gupta D, Lis CG (2009). Role of CA125 in predicting ovarian cancer survival - a review of the epidemiological literature. *J Ovarian Res*. 2: 13.

Hanson PI, Cashikar A (2012). Multivesicular body morphogenesis. *Annu Rev Cell Dev Biol*. 28: 337-362.

Hellstern S, Sasaki T, Fauser C, Lustig A, Timpl R, Engel J (2002). Functional studies on recombinant domains of Mac-2-binding protein. *J Biol Chem*. 277: 15690-15696.

Henne WM, Buchkovich NJ, Emr SD (2011). The ESCRT pathway. *Dev Cell*. 21: 77-91.

Jelovac D, Armstrong DK (2011). Recent progress in the diagnosis and treatment of ovarian cancer. *CA Cancer J Clin*. 61: 183-203.

Kalra H, Simpson RJ, Ji H, Aikawa E, Altevogt P, Askenase P, Bond VC, Borras FE, Breakefield X, Budnik V, Buzas E, Camussi G, Clayton A, Cocucci E, Falcon-Perez JM, Gabrielsson S, Gho YS, Gupta D, Harsha HC, Hendrix A, Hill AF, Inal JM, Jenster G, Kramer-Albers EM, Lim SK, Llorente A, Lotvall J, Marcilla A, Mincheva-Nilsson L, Nazarenko I, Nieuwland R, Nolte-'t Hoen EN, Pandey A, Patel T, Piper MG, Pluchino S, Prasad TS, Rajendran L, Raposo G, Record M, Reid GE, Sanchez-Madrid F, Schiffelers RM, Siljander P, Stensballe A, Stoorvogel W, Taylor D, Thery C, Valadi H, van Balkom BW, Vazquez J, Vidal M, Wauben MH, Yanez-Mo M, Zoeller M, Mathivanan S (2012). Vesiclepedia: a compendium for extracellular vesicles with continuous community annotation. *PLoS Biol*. 10: e1001450.

Karst AM, Drapkin R (2010). Ovarian cancer pathogenesis: a model in evolution. *J Oncol*. 2010: 932371.

Keller S, Konig AK, Marme F, Runz S, Wolterink S, Koensgen D, Mustea A, Sehouli J, Altevogt P (2009). Systemic presence and tumor-growth promoting effect of ovarian carcinoma released exosomes. *Cancer Lett*. 278: 73-81.

Kourembanas S (2015). Exosomes: vehicles of intercellular signaling, biomarkers, and vectors of cell therapy. *Annu Rev Physiol*. 77: 13-27.

Kowal J, Tkach M, Thery C (2014). Biogenesis and secretion of exosomes. *Curr Opin Cell Biol*. 29: 116-125.

Lamparski HG, Metha-Damani A, Yao JY, Patel S, Hsu DH, Ruegg C, Le Pecq JB (2002). Production and characterization of clinical grade exosomes derived from dendritic cells. *J Immunol Methods*. 270: 211-226.

Liang Y, Eng WS, Colquhoun DR, Dinglasan RR, Graham DR, Mahal LK (2014). Complex N-linked glycans serve as a determinant for exosome/microvesicle cargo recruitment. *J Biol Chem*. 289: 32526-32537.

Machado E, Kandzia S, Carilho R, Altevogt P, Conradt HS, Costa J (2011). N-Glycosylation of total cellular glycoproteins from the human ovarian carcinoma SKOV3 cell line and of recombinantly expressed human erythropoietin. *Glycobiology*. 21: 376-386.

Marleau AM, Chen CS, Joyce JA, Tullis RH (2012). Exosome removal as a therapeutic adjuvant in cancer. *J Transl Med*. 10: 134.

Mechtersheimer S, Gutwein P, Agmon-Levin N, Stoeck A, Oleszewski M, Riedle S, Postina R, Fahrenholz F, Fogel M, Lemmon V, Altevogt P (2001). Ectodomain shedding of L1 adhesion molecule promotes cell migration by autocrine binding to integrins. *J Cell Biol*. 155: 661-673.

Melo SA, Luecke LB, Kahlert C, Fernandez AF, Gammon ST, Kaye J, LeBleu VS, Mittendorf EA, Weitz J, Rahbari N, Reissfelder C, Pilarsky C, Fraga MF, Piwnica-Worms D, Kalluri R (2015). Glypican-1 identifies cancer exosomes and detects early pancreatic cancer. *Nature*. 523: 177-182.

Mo D, Costa SA, Ihrke G, Youker RT, Pastor-Soler N, Hughey RP, Weisz OA (2012). Sialylation of N-linked glycans mediates apical delivery of endolyn in MDCK cells via a galectin-9-dependent mechanism. *Mol Biol Cell*. 23: 3636-3646.

Moremen KW, Tiemeyer M, Nairn AV (2012). Vertebrate protein glycosylation: diversity, synthesis and function. *Nat Rev Mol Cell Biol*. 13: 448-462.

Nordin JZ, Lee Y, Vader P, Mager I, Johansson HJ, Heusermann W, Wiklander OP, Hallbrink M,
Seow Y, Bultema JJ, Gilthorpe J, Davies T, Fairchild PJ, Gabrielsson S, Meisner-Kober NC, Lehtio J, Smith CI, Wood MJ, El Andaloussi S (2015). Ultrafiltration with size-exclusion liquid chromatography for high yield isolation of extracellular vesicles preserving intact biophysical and functional properties. *Nanomedicine*. 11: 879-883.

Pilobello KT, Slawek DE, Mahal LK (2007). A ratiometric lectin microarray approach to analysis of the dynamic mammalian glycome. *Proc Natl Acad Sci U S A*. 104: 11534-11539.

Pinho SS, Reis CA (2015). Glycosylation in cancer: mechanisms and clinical implications. *Nat Rev Cancer*. 15: 540-555.

Raposo G, Stoorvogel W (2013). Extracellular vesicles: exosomes, microvesicles, and friends. *J Cell Biol*. 200: 373-383.

Sasaki T, Brakebusch C, Engel J, Timpl R (1998). Mac-2 binding protein is a cell-adhesive protein of the extracellular matrix which self-assembles into ring-like structures and binds beta1 integrins, collagens and fibronectin. *EMBO J*. 17: 1606-1613.

Seberger PJ, Chaney WG (1999). Control of metastasis by Asn-linked, beta1-6 branched oligosaccharides in mouse mammary cancer cells. *Glycobiology*. 9: 235-241.

Skog J, Wurdinger T, van Rijn S, Meijer DH, Gainche L, Sena-Esteves M, Curry WT, Jr., Carter BS, Krichevsky AM, Breakefield XO (2008). Glioblastoma microvesicles transport RNA and proteins that promote tumour growth and provide diagnostic biomarkers. *Nat Cell Biol*. 10: 1470-1476.

Song Y, Aglipay JA, Bernstein JD, Goswami S, Stanley P (2010). The bisecting GlcNAc on N-glycans inhibits growth factor signaling and retards mammary tumor progression. *Cancer Res*. 70: 3361-3371.

Stampolidis P, Ullrich A, Iacobelli S (2015). LGALS3BP, lectin galactoside-binding soluble 3 binding protein, promotes oncogenic cellular events impeded by antibody intervention. *Oncogene*. 34: 39-52.

Stoeck A, Keller S, Riedle S, Sanderson MP, Runz S, Le Naour F, Gutwein P, Ludwig A, Rubinstein E, Altevogt P (2006). A role for exosomes in the constitutive and stimulus-induced ectodomain cleavage of L1 and CD44. *Biochem J*. 393: 609-618.

Stowell SR, Ju T, Cummings RD (2015). Protein glycosylation in cancer. *Annu Rev Pathol*. 10: 473-510.

Szajnik M, Derbis M, Lach M, Patalas P, Michalak M, Drzewiecka H, Szpurek D, Nowakowski A, Spaczynski M, Baranowski W, Whiteside TL (2013). Exosomes in Plasma of Patients with Ovarian Carcinoma: Potential Biomarkers of Tumor Progression and Response to Therapy. *Gynecol Obstet (Sunnyvale)*. Suppl 4: 3.

Taylor DD, Shah S (2015). Methods of isolating extracellular vesicles impact down-stream analyses of their cargoes. *Methods*.

Taylor ME, Drickamer K (2011). Introduction to Glycobiology. New York, Oxford University Press.

Torre LA, Bray F, Siegel RL, Ferlay J, Lortet-Tieulent J, Jemal A (2015). Global cancer statistics, 2012. *CA Cancer J Clin*. 65: 87-108.

Trajkovic K, Hsu C, Chiantia S, Rajendran L, Wenzel D, Wieland F, Schwille P, Brugger B, Simons M (2008). Ceramide triggers budding of exosome vesicles into multivesicular endosomes. *Science*. 319: 1244-1247.

Vader P, Breakefield XO, Wood MJ (2014). Extracellular vesicles: emerging targets for cancer therapy. *Trends Mol Med*. 20: 385-393.

Varki A, Cummings RD, Esko JD, Freeze HH, Stanley P, Bertozzi CR, Hart GW, Etzler ME (2009). Essentials of Glycobiology. New York, Cold Spring Harbor Laboratory Press.